R010-01
C 会場 ：11/4　PM1 （13:45-15:30）
13:45〜14:00

開放上流境界条件におけるテアリング不安定性の線形理論

#清水　徹 [1)]
([1]RCSCE, 愛媛大

Linear Theory of Tearing Instability for open upstream boundary conditions

#Tohru Shimizu[1)]
([1]RCSCE, Ehime Univ.

For resistive MHD instability of a current sheet which is driven by magnetic reconnection process, some recent developments of the linear theory is comprehensively reported. By numerically solving the perturbation equations derived in the theory, author modified and improved the previous standard theories (FKR1963 and LSC2007). The recent studies are being shifted to the introductions of viscosity effect and hyper resistivity effect and also the improvement of the WKB approximation used in LSC2007. In this talk, those three topics are totally reported in Japanese.

磁気再結合過程による電流層の抵抗性 MHD 不安定性について MHD 線形理論の最近の研究成果を包括的に報告する。初期値問題として数値的に摂動方程式を解くことで、講演者は従来の二つの標準理論 (FKR1963,LSC2007) を根本的に修正した。最近の研究は、粘性効果や HyperResistivity 効果の導入や WKB 近似の高精度化へと移行している。直近の 3 つの国際会議における講演者の発表 (AOGS2022, ICNSP2022, AAPPS-DPP2022) を日本語で包括的に説明する。今後の研究の方向性についても議論したい。

R010-02
C 会場 ：11/4　PM1 （13:45-15:30）
14:00〜14:15

#殷　振興 [1)], 大村　善治 [1)]
([1] 京都大学大村研究室

Dependence of nonlinear wave growth of hiss emissions on the gradient of the magnetic field and thermal fluctuation

#ZHENXING YIN[1)], Yoshiharu Omura[1)]
([1]Kyoto University Omura laboratory

Dependence of nonlinear wave growth of whistler-mode hiss emissions on the gradient of the magnetic field and thermal fluctuation in the plasmasphere

Zhen-Xing Yin and Yoshiharu Omura
Research Institute for Sustainable Humanosphere, Kyoto University

We perform a series of electromagnetic particle simulations in the magnetospheric plasma for studying the nonlinear wave growth of the generation of hiss emissions. We examin two parameters, which are the number of hot and cold super-particles and the gradient of the background magnetic field. Firstly we vary the gradient of the background magnetic field from zero and increase it. We find that in the case of the zero gradient the wave amplitude attains the smallest value compared with other cases of finite gradients. There is an optimum value with which wave amplitudes grow to the largest value. The amplitude starts to decrease with a gradient greater than the optimum value. With a gradient less than the optimum value, the nonlinear wave growth process is promoted, while the gradient is greater than the optimum value the nonlinear wave growth is suppressed. We also studied cases of different magnetic field gradients and different numbers of super-particles. We find that wave amplitudes take larger values with a smaller number of super-particles. Many wave packets are generated, which looks like hiss emissions.

When we increase the number of super-particles keeping the hot plasma frequency constant, the charge q of a super-particle is decreased which results in a decreased level of thermal fluctuation. Starting from the smaller wave amplitude, the number of growing wave packets are decreased, while the growth rates of wave packets become larger, resulting in discrete waves like chorus emissions.

References:

[1] Hikishima, M., Omura, Y., Summers, D. (2020), Particle simulation of the generation of plasmaspheric hiss. Journal of Geophysical Research: Space Physics, 125, e2020JA027973, https://doi.org/10.1029/2020JA027973.

[2] Liu, Y., Omura, Y., Hikishima, M. (2021), Simulation study on parametric dependence of whistler - mode hiss generation in the plasmasphere, Earth, Planets and Space 73, 230.

[3] Liu, Y., & Omura, Y. (2022). Nonlinear wave growth of whistler-mode hiss emissions in a uniform magnetic field. Journal of Geophysical Research: Space Physics, 127, e2022JA030428.

R010-03
C 会場 ：11/4　PM1 （13:45-15:30）
14:15〜14:30

#村瀬　清華 [1)], 片岡　龍峰 [1,2)], 西山　尚典 [1,2)], 佐藤　薫 [3)], 堤　雅基 [2)], 田中　良昌 [1,2,4)], 小川　泰信 [1,2)]
([1] 総研大・極域科学,([2] 極地研,([3] 東大・理,([4]ROIS-DS

Evaluation of atmospheric ionization by X-rays, solar protons, and radiation belt electrons in September 2017 space weather event

#Kiyoka Murase[1)], Ryuho Kataoka[1,2)], Takanori Nishiyama[1,2)], Kaoru Sato[3)], Masaki Tsutsumi[2)], Yoshimasa Tanaka[1,2,4)], Yasunobu Ogawa[1,2)]
([1]Polar Science, SOKENDAI,([2]NIPR,([3]Graduate School of Science, Univ. of Tokyo,([4]ROIS-DS,

On September 11, 2017, when the solar proton flux peaked at the geostationary orbit, the PANSY radar at Syowa Station observed mesospheric echoes at 42 km, the lowest altitude ever observed. The estimated ionization rate by PHITS (Particle and Heavy Ion Transport code System) air-shower simulation with the proton flux obtained by the GOES satellite peaked at ˜40 km, suggesting that the echo power is enhanced by the increase in electron density due to proton precipitation. The intensity of cosmic noise absorption (CNA) from the resultant ionization rate was ˜2.8 dB, which consistently explains the maximum intensity of observed CNA level of ˜3.0 dB. Further, we used the X-ray flux observed by the GOES satellite as the input data for PHITS to estimate the electron density enhancements as observed by the EISCAT radar at Tromso, Norway due to the two X-class flare events at ˜9 and ˜12 UT on September 6. Obtained density profiles and the time sequence are roughly consistent with the observed EISCAT data, within the error of a factor of two. At ˜1345 UT on September 6, a transient low-altitude PANSY echo at $<$50 km and CNA spike (˜2.0 dB) were accompanied by Pc1 geomagnetic pulsations, which can be a dayside relativistic electron precipitation event associated with EMIC waves. The ionization rate due to the energetic electrons is also evaluated by PHITS with the inputs from NOAA MEPED electron data, and the observed CNA level of ˜2.0 dB can be reproduced by the contribution of sub-MeV electrons. We conclude that the September 2017 space weather event with the cutting-edge space-borne and ground-based observations provides a rare opportunity to cross-validate the use of PHITS simulation with different types of inputs (X-rays, protons, and electrons) to evaluate the atmospheric ionization.

R010-04
C 会場 ：11/4　PM1 （13:45-15:30）
14:30〜14:50

宇宙天気研究と機械学習の現状や今後の展望

#片岡　龍峰 [1)]
(1 極地研

Current status and future prospects of space weather research and machine learning

#Ryuho Kataoka[1)]
(1NIPR

Machine learning techniques have been broadly utilized in space weather forecast. We introduce an application example of a machine learning technique called Echo State Network (ESN) to reconstruct solar wind data for several extreme magnetic storms for which little or no solar wind data were previously available (doi.org/10.1029/2021GL096275). We also introduce other examples of the same technique to substorm predictions (doi.org/10.5194/angeo-40-11-2022) and calibration of galactic cosmic rays measurements (doi.org/10.31223/X5PW6V). Based on the experience, we discuss the current status and future prospects of space weather research and machine learning.

機械学習技術は、宇宙天気予報で広く利用されている。一例として、以前は太陽風データがほとんどまたはまったく利用できなかったいくつかの極端な磁気嵐の太陽風データを再構築できる、エコーステートネットワーク（ESN）と呼ばれる機械学習技術のアプリケーションを紹介する（doi.org/10.1029/2021GL096275）。また、サブストーム予測（doi.org/10.5194/angeo-40-11-2022）や、銀河宇宙線計測のキャリブレーション（doi.org/10.31223/ X5PW6V）に同様の手法を用いた例についても紹介する。これらの経験に基づいて、宇宙天気研究と機械学習の現状と将来の展望について議論する。

R010-05
C 会場 ：11/4　PM1 （13:45-15:30）
14:50〜15:05

太陽フレア予測モデル Deep Flare Net の改良への試み

#宇都宮　惇典 [1)], 銭谷　誠司 [2)], 西塚　直人 [3)], 久保　勇樹 [3)]
[(1] 神戸大学,[(2] 神戸大学,[(3] 情報通信研究機構

Attempts to improve the solar flare prediction model Deep Flare Net

#Atsunori Utsunomiya[1)], Seiji Zenitani[2)], Naoto Nishizuka[3)], Yuki Kubo[3)]
[(1]Kobe University,[(2]Kobe U,[(3]NICT

In recent years, solar flares occurring on the solar surface are thought to have the potential to cause large-scale power outages and long-lasting communication disruptions. That is why predicting solar flares in advance is important for disaster countermeasure against telecommunications and other disasters. In 2018, Nishizuka et al. at NICT developed a solar flare prediction model called Deep Flare Net (DeFN) to achieve highly accurate flare prediction. The DeFN is a model that predicts the largest flares that will occur within 24 hours based on 79 features such as maximum X-ray intensity and the number of magnetic neutral lines observed on the solar surface.

In this study, we investigate the importance of each feature to improve the performance of DeFN for better solar flare prediction. We also apply the current 1-day prediction to half-day and 2-day flare occurrence predictions to see if the accuracy can be maintained. DeFN is the latest prediction model developed in 2018, these attempts could lead to model improvements. We will report on these results.

近年、太陽表面上で発生している太陽フレアが大規模停電や長時間の通信障害を引き起こす可能性があると考えられている。そのため太陽フレアを事前に予測することが、通信などへの災害対策にとって重要である。太陽フレア予測の研究では、2018 年に NICT の西塚らが Deep Flare Net (DeFN) という太陽フレア予測モデルを開発して、高精度のフレア予測を実現した。DeFN とは太陽表面で観測される最大 X 線強度や磁気中性線の本数などの 79 種類の特徴量をもとに 24 時間以内に起きる最大規模のフレア発生を予測するモデルである。

本研究では、太陽フレア予測の改善に繋げるために、DeFN の性能向上に向けて特徴量ごとの重要度を調査した。また、現在の 1 日後の予測を半日後や 2 日後のフレア発生予測にも応用し、精度を維持できるかも検証を進めている。DeFN は 2018 年に開発された最新の予測モデルであるため、これらの試みはモデルの改良に繋がる可能性がある。今回はこれらの検証成果について報告する。

R010-06
C 会場 ：11/4　PM1 （13:45-15:30）
15:05〜15:20

機械学習を用いた太陽 EUV 放射スペクトルの予測

#前田　護 [1)], 渡邉　恭子 [1)], 西本　将平 [1)], 北島　慎之典 [1)], 下条　圭美 [2)], 行方　宏介 [3)], 増田　智 [4)]
([1] 防衛大,[2] 国立天文台・チリ観測所,[3] 国立天文台,[4] 名大

Prediction of Solar EUV Emission Spectrum Using Machine Learning

#Mamoru Maeda[1)], Kyoko Watanabe[1)], Shohei Nishimoto[1)], Shinnosuke Kitajima[1)], Masumi Shimojo[2)], Kosuke Namekata[3)], Satoshi Masuda[4)]
([1]NDA,[2]Chile Observatory, NAOJ,[3]NAOJ,[4]Nagoya U.,

X-ray (0.1-10 nm) and extreme ultraviolet (EUV: 10-124 nm) emissions from the Sun ionize atoms and molecules in the Earth's upper atmosphere and contribute to the formation of the ionosphere. The ionosphere is used for satellite and terrestrial communications, and since the ionospheric environment fluctuates with the 11-year solar cycle and sudden space weather phenomena such as solar flares, it is necessary to monitor and predict the ionospheric environment to keep a stable communication environment.

The effects of solar X-rays and EUV emissions on the ionosphere are not known precisely because these emissions are observed by satellites, and satellites data are limited both in duration and resolution of observations. On the other hand, since microwave emissions from the Sun can be observed on the ground, especially microwave observation at 2.8 GHz (F10.7) have traditionally been used as proxies for EUV emission when estimating the impact of solar emissions on the Earth's upper atmosphere. However, recent satellite observations of EUV emission spectra have shown that there is a discrepancy in the flux variation between F10.7 and the EUV emission spectra.

In this study, we investigate the solar cycle variation of the relationship between microwave and EUV emission spectra using data from the Nobeyama Radio Polarimeters (NoRP) and Thermosphere · Ionosphere · Mesosphere · Energetics and Dynamics (TIMED)/Solar Extreme ultraviolet Experiment (SEE). The NoRP measures the flux of microwave emissions from the full Sun at multiple frequencies (1, 2, 3.75, 9.4 GHz), and TIMED/SEE measures 0.5-190 nm EUV emission spectra with a resolution of 1 nm. When we use daily data and investigated the relationship between them, all frequencies of microwave emissions had good correlations with EUV radiation spectra, however, lower frequency emissions tended to have a better correlation with EUV emissions. In addition, the correlation tended to be worse especially in the EUV wavelength band which contains a large amount of line emissions from the chromosphere, and the slope of the correlation also differed.

It is difficult to accurately derive the relationship between microwave frequency and EUV emission spectra only by comparing the observed data, because the emission mechanisms of microwave and EUV emissions are different. Therefore, we reproduced solar EUV emission spectra from multiple frequencies of microwave observations using a machine learning method with reference to Zhang & Paxton (2018). The input microwave data to machine learning were not only the NoRP data mentioned above, but also the Learmonth solar radio telescopes monitor data which was used in Zhang & Paxton (2018) (245, 440, 610, 1415, 2695, 4995, 8800, 15400 MHz) were used. Using daily observations between 2002 and 2016, we reproduced several EUV wavelength bands (e.g., 13.5, 30.5, 121.5 nm) obtained with TIMED/SEE and found that none of the EUV bands are well reproduced and had correlation coefficients of 0.97 or higher. However, it was not possible to identify the frequency of the microwave that is mainly responsible for the EUV emission spectrum, and the results showed that machine learning can be used to reproduce the EUV emission spectrum at any frequency.

In this presentation, the relationship between microwave and EUV emissions during solar activity cycles will be discussed using data analysis and machine learning results.

太陽からの X 線（0.1-10 nm）と極紫外線（EUV: 10-124 nm）放射は、地球上層大気中の原子や分子を電離し、多量の電子やイオンを生成することにより、電離圏の形成に寄与している。電離圏は衛星通信や地上の通信で利用されているが、電離圏の環境は太陽の 11 年周期や太陽フレアなどの突発的な現象によって変動するため、安定した通信環境確保のために、電離圏環境を監視・予測することが必要となっている。

太陽放射の電離圏への影響は、太陽 X 線・EUV が人工衛星を用いて観測されており観測データが少ないことから、正確には分かっていない。一方、太陽からの放射のうち電波は地上で観測できるため、地球圏環境への太陽放射の影響を見積もる時には F10.7 という 2.8 GHz の電波が EUV 放射のプロキシとして用いられてきた。しかし、近年の EUV 放射スペクトルの衛星観測などにより、F10.7 だけでは実際に地球圏環境に影響している放射を説明できないことが分かってきた。

そこで、太陽周期変動による電波放射と EUV 放射スペクトルの関係の変動について、野辺山強度偏波計 (NoRP) と TIMED/SEE のデータを用いて調べた。NoRP は太陽全体からの電波強度を多周波 (1, 2, 3.75, 9.4 GHz) で測定しており、TIMED/SEE は 0.5-190 nm の EUV 放射スペクトルを 1 nm の分解能で 1 日に 15 回測定している。これらの電波放射と EUV 放射の関係を調べたところ、どの周波数の電波も EUV 放射スペクトルと良い相関が見られたが、低周波数の電波放射の方が EUV 放射との相関が良い傾向が見られた。また、彩層からのライン放射を多く含む EUV 放射チャンネルで相関が悪くなり、傾きも変化している様相が見られた。

電波放射と EUV 放射では放射機構が異なることから、これらの放射の関係を観測データの比較のみから正確に導出することは難しい。そこで本研究では、Zhang & Paxton (2018）を参考にして、機械学習を用いて複数周波数の電波観測データから特定の太陽 EUV 放射スペクトルの再現をおこなった。入力の電波データは、上記の NoRP のデータのみならず、Zhang & Paxton (2018）で用いられていたオーストラリアの Learmonth solar radio telescopes monitor の観測データ（245, 440, 610, 1415, 2695, 4995, 8800, 15400 MHz）も使用した。2002 年から 2016 年の間の日観測データを用いて、TIMED/SEE で得られた太陽 EUV 放射スペクトルのうちいくつかの波長バンド（13.5, 30.5, 121.5 nm など）の再現を行ったところ、どの EUV 放射も相関係数 0.97 以上で再現することができた。しかし、EUV 放射スペクトルに主に効いている電波の周波数は特定することができず、機械学習を用いれば、どの周波数の電波でも EUV 放射スペクトル再現できるという結果が得られた。

今回の発表では、これらの太陽活動周期における電波放射と EUV 放射の関係について、データ解析と機械学習の結果を用いて議論する。

R010-07
C 会場 ：11/4　PM2 （15:45-18:15）
15:45〜16:20

宇宙天気・宇宙気候研究のこれまでとこれから

#塩川　和夫 [1)]
(1 名大宇地研

Current and possible future direction of space weather and space climate research

#Kazuo Shiokawa[1)]
(1ISEE, Nagoya Univ.

Research on space weather and space climate in Japan has developed in various areas of ground-based and satellite observations and simulations, starting with the former Radio Research Laboratory and Communications Research Laboratory (currently the National Institute of Information and Communications Technology). In the satellite program, while the main objectives of Akebono (1989-2015) and Geotail (1992-) were auroral acceleration mechanisms and magnetospheric tail science issues, respectively, the main objective of the Arase satellite (2016-) was radiation belt particle acceleration mechanisms, which led to a strong application to space weather and space climate research, such as space weather forecasts and the effects of high-energy particles on atmospheric environments. The concept of space weather and space climate for short-term and long-term variability has become popular since CAWSES (2003-2008, Climate and Weather of the Sun-Earth System) and CAWSES-II (2009-2013) promoted by the Scientific Committee on Solar-Terrestrial Physics (SCOSTEP) under the International Science Council. This concept has led to VarSITI (2014-2018, Variability of the Sun and Its Terrestrial Impact) and PRESTO (2020-2024, Predictability of the variable Solar-Terrestrial Coupling). The importance of space weather research is increasing as space applications such as satellite positioning and satellite communications expand. The fall of 40 StarLink satellites in February of this year due to a magnetic storm is still fresh in our memory. In Japan, the Ministry of Internal Affairs and Communications (MIC) held 10 meetings this year to discuss ways to advance space weather forecasting, and Japan issued their first official document on space weather forecasting, which has been widely reported and has attracted public attention to space weather. In the future, the challenge will be how to connect this research on space weather and space climate with users as a familiar disaster response issue in society. On the research side, one important issue will be to clarify the dynamical and chemical response of the Earth's atmosphere to the energy input from space.

日本の宇宙天気・宇宙気候の研究は、旧電波研究所・通信総合研究所（現情報システム研究機構）をはじめとして、地上観測や人工衛星観測、シミュレーションのさまざまな領域で発達してきた。人工衛星計画では、あけぼの (1989-2015)、Geotail(1992-) がオーロラ加速機構や磁気圏尾部の科学課題を主目的に据えてきたのに対し、あらせ衛星 (2016-) では放射線帯粒子加速機構を主目的に据えたために、宇宙天気予報や高エネルギー粒子の大気環境への影響など、宇宙天気・宇宙気候研究への応用的な側面が強く出されるようになった。国際的には、この分野の国際組織である太陽地球系物理学科学委員会（SCOSTEP）が 2003-2008, 2009-2013 に推進した CAWSES, CAWSES-II（太陽地球系の気候と天気）から、短期変動と長期変動に対する宇宙天気・宇宙気候という概念が一般的になり、この考え方は VarSITI（2014-2018, 太陽活動変動とその地球への影響)、PRESTO（2020-2024、変動する太陽地球結合系の予測可能性）へとつながっている。衛星測位や衛星通信などの宇宙利用が拡大するにつれて、宇宙天気研究の重要性はますます増加している。今年 2 月の磁気嵐に伴う StarLink 衛星 40 機の落下は記憶に新しい。日本では総務省による「宇宙天気予報の高度化の在り方に関する検討会」が今年 10 回にわたって開催され、日本の国として初めて、宇宙天気予報に関する文書が出されて報道も拡がり、宇宙天気に関する注目が集まっている。今後は、この宇宙天気や宇宙気候の研究を社会の身近な災害対応課題として、ユーザーとの間をいかにつないでいくかが課題となっていくであろう。また研究の側面では、宇宙からのエネルギー流入に対する地球大気の力学・化学的な応答を明らかにしていくことが一つの重要な課題であると思われる。

R010-08
C 会場 ：11/4　PM2 （15:45-18:15）
16:20〜16:35

太陽-地球方向を向いた惑星間空間磁場に対する地球磁気圏の応答研究

#城戸　蓮太郎 [1)], 吉川　顕正 [2,3)], 魚住　禎司 [2)]
[(1] 九州大学　大学院理学府,[(2] 国際宇宙惑星環境研究センター・アイスペース,[(3] 九州大学・理学研究院

Study of the response of the Earth's magnetosphere to a Sun-Earth oriented interplanetary magnetic field

#Rentaro Kido[1)], Akimasa Yoshikawa[2,3)], Teiji Uozumi[2)]
[(1]Kyushu University,[(2]International Research center for Space and Planetary Environmental Science ・i-SPES,[(3]Kyushu Univ.

Many studies have been conducted on the response of the Earth's magnetosphere to the Interplanetary Magnetic Field (IMF). In particular, the study of the dependence of the magnetic reconnection between the solar wind and the Earth's magnetic field on the z-component (north-south component) of the IMF has been one of the key issues in space weather research. On the other hand, the dependence of the IMF on the y-component (east-west component), which is known to produce a torque that twists the Earth's magnetotail during magnetic reconnection, has also been studied extensively. Since the IMF dependence on the magnetospheric response has been considered to be largely due to the z/y component, there has been little systematic investigation of the effect of the x component of the IMF (sun-Earth component) on the Earth's magnetosphere as a control parameter, and the physical effects of this effect are not clear. For example, K. M. Laundal, et al. (2017) found in a computer experiment by S. Hoilijoki, et al. (2014) that the dominant effect of the IMF x component is to change the overall energy conversion efficiency between the solar wind and the magnetosphere due to reconnection. However, most previous studies, including this view, have focused on macroscopic analyses of magnetospheric physics using global simulators, and little progress has been made in observational data-based investigations of the effects of the IMF x component.

In order to overcome this situation, we are carrying out an observation-based study to clarify the impact of the IMF x-component on the magnetospheric-ionospheric coupling system. In this presentation, we will report the initial results of our investigation of the effects on various space weather parameters (e.g., AL index) and the horizontal equivalent current system of the Ampere Map, using a method to objectively extract situations in which only the x-component approaches the Earth with a strong IMF.

惑星間空間磁場（Interplanetary Magnetic Field : IMF）に対する地球磁気圏の応答について、これまで多くの研究が積み重ねられてきた。特に、太陽風と地球磁場の磁気再結合の制御に関する、IMF の z 成分（南北方向成分）依存性の研究は、宇宙天気研究の中心課題の 1 つである。一方で磁気再結合の際に、地球磁気圏尾部を捻る形のトルクを生むことが知られている、IMF の y 成分（東西方向成分）依存性に関しても、多くの研究が行われている。地球磁気圏応答に関する IMF 依存性は、こうした z/y 成分の影響が大きいとされてきたため、IMF の x 成分（太陽-地球方向成分）をコントロールパラメーターとした地球磁気圏への影響に対する系統的な調査は殆ど進んでおらず、それが及ぼす物理的効果も明確ではない。例えば、K. M. Laundal, et al.（2017）では、S. Hoilijoki, et al.（2014）の計算機実験で見いだされた、IMF x 成分の支配的な効果は、リコネクションによる太陽風と磁気圏の間の全体的なエネルギー変換効率を変化させることにあるとしている。しかしながら、この見解を含めた先行研究の多くは、グローバルシミュレーターを用いた磁気圏物理の巨視的な解析が中心であり、観測データをベースとした、IMF x 成分がもたらす影響に関する調査は殆ど進んでいない。

このような状況を打破するため、我々は、IMF x 成分による地球磁気圏-電離圏結合システムへの影響を明らかにすることを目的とした、観測データに基づく調査・研究を遂行している。本発表では、x 成分のみが強い IMF を持って地球に接近する状況を客観的に抽出する手法を用いて、さまざまな宇宙天気パラメータ、（例えば AL index 等）や Ampere Map の水平等価電流系にどのような影響が及ぼされるのかについて調査した初期結果について報告する。

R010-09
C 会場 ：11/4　PM2 （15:45-18:15）
16:35〜16:50

時空発展する 3 次元磁場ベクトル場記述のためのアフィン接続

#吉川　顕正 [1)]
(1 九大/理学研究院

Development of Affine Connection for Describing Spatiotemporal Evolving 3D Magnetic Vector Fields

#Akimasa Yoshikawa[1)]
(1Kyushu Univ.

We have developed an affine connection on a differentiable manifold for analyzing and formulating the geometrical structure of magnetic fields as vector fields evolving arbitrarily in space-time.

A manifold is a space that can define a local Euclidean space at all points belonging to it. At each point on the manifold, a tangent space (tangent vector space) is defined. The tangent vector space is the set of all tangent vectors passing through the points of contact, forming a tangent vector field. This tangent vector field can be assumed to be a variety of calculus laws established in Euclidean space in the vicinity of the points of contact on the manifold. By ”connecting” the tangent vector space defined at each of these points with the surrounding tangent vector space by a parallel shift on the manifold, the vector field in the entire space on the manifold can be defined. This ”connection” of tangent vector spaces by parallel shifts on the manifold is an affine connection. That is, the affine connection allows the tangent vector field defined at each point on the manifold to behave like a function with values in the vector space fixed at each point. In other words, a collection of local coordinate systems defined at each point on the manifold covers the entire space, and data and physics can be described and compared under a common rule.

The affine connection we have developed enables us to capture the vector field as a fiber bundle of tightly distributed magnetic field lines and to describe its geometrical structure in the framework of ordinary vector analysis.This method extends the locally defined orthonormal Cartesian coordinate system parallel and perpendicular to the magnetic field in 3D by the following methodology:

(1) . To investigate the geometry of magnetic field lines, we first introduce the Frenet frame, which is a dynamic frame along a single curved line.In the Frenet frame, the local principal curve direction is determined by the unit vector in the tangent direction of the curve of interest, and the unit vectors in the principal normal (curvature direction) and secondary normal (orthogonal to the above two) directions to the principal curve are used to form a ”local normal orthogonal system ” is formed. Considering a tightly distributed group of magnetic field lines, this local normal orthogonal system will be distributed in space.

(2) . To connect the local orthonormal orthogonal systems distributed in this space, vector curved lines formed by connecting unit vectors in the main normal and bi-normal directions are introduced, and by shifting along each curve, the relative relationship with adjacent magnetic field lines is grasped and the analytical space is extended to the entire system.

(3). (1) and (2) uniquely determine the distribution of curvature and twist ratio for each curve filling the space tightly. This determines how the ”tetrahedron” formed by the local orthonormal basis changes along with each curve (rigid directional change and rotation), and the 3-dimensional geometric structure of the magnetic field is completely determined.

That is, by shifting the tetrahedron formed by the local coordinate system along the principal curve, the principal normal, and the bi-normal, respectively, we can understand how the moving tetrahedron curved and rotated along the curved line, thereby determining the structure of the vector field that extends over the entire space. This is a methodology to know the structure of the vector field expanding in the whole space. Furthermore, the temporal evolution ratio of this tetrahedron (temporal changing ratio of direction and twisting ratio) is derived. This allows us to describe the 3-dimensional evolution of the magnetic field geometry.

In the talk, we will give an overview of the fundamental structure of the vector field obtained by these frameworks and discuss the underlying physics-based determinants of the vector field.

任意に時空発展するベクトル場としての磁場の幾何学的構造を解析・定式化するための可微分多様体上のアフィン接続を開発した。多様体とは、それに属するすべての点において、「局所的なユークリッド空間を定義出来る空間」のことである。多様体上の各点では、接空間（接ベクトル空間）が定義される。接ベクトル空間は、接点を通るすべての接ベクトルの集合であり、接ベクトル場を形成する。この接ベクトル場は、多様体上の接点近傍では、ユークリッド空間で成立する様々な微積分則が成り立つとすることが出来る。この各点で定義される接ベクトル空間を「多様体上の平行移動によって、周囲の接ベクトル空間と＜接続＞する」ことにより、多様体上の全空間におけるベクトル場が定義される。この多様体上の平行移動による接ベクトル空間の＜接続＞が、アフィン接続である。即ち、アフィン接続により、多様体上の各点で定義される接ベクトル場が、各点で固定されたベクトル空間に値をもつ関数のように振る舞うことが可能となる。言い

換えれば、多様体上の各点で定義された、局所座標系を連ねることにより全空間を覆い、共通のルールの下、データや物理を記述・比較することが可能となる。

我々開発したアフィン接続では、ベクトル場を稠密に分布する磁力線を束ねたファイバー束として捉え、その幾何学構造を通常のベクトル解析のフレームワークで記述することを可能とする。本手法では、以下の方法論により、局所的に定義される磁場と平行方向・垂直方向の正規直交座標系を 3 次元拡張し、全空間でのベクトル場の解析を可能とする。

（1）磁力線の幾何を調べるためにまず、1 本の曲線に沿った動標講である Frenet 標構を導入する。Frenet 標構では、着目する曲線（主曲線）の接線方向の単位ベクトルにより、局所的な主曲線方向を定め、その主曲線に対する主法線方向（曲率方向)、従法線方向（上記 2 者と直交する方向）の単位ベクトルを用いて、“局所正規直交系”を形成する。系に稠密に分布する磁力線群を考慮すると、この局所正規直交系は、空間上に分布することになる。

（2）この空間にばらまかれた、局所正規直交系の接続を行う為に、主法線方向、従法線方向の単位ベクトルを連ねて形成されるベクトル曲線を導入し、それぞれの曲線に沿って平行移動することにより、隣接する磁力線との相対関係を把握するとともに、解析空間を系全体へと拡張する。

（3）(1)（2）により、空間を稠密に満たした各曲線の、曲率と捻れ率の分布が一意決定される。これにより、局所正規直交基底で形成される“正 4 面体”が、各曲線に沿って変化する様子（剛体的な方向変化と回転）が決定され、磁場の 3 次元的な幾何構造が、完全に決定される。

即ち、局所座標系が張る 4 面体を、主曲線、主法線、従法線それぞれの方向に沿って変位させることにより、この動 4 面体が、どのように曲線に沿って曲がり、回転するのかを把握することにより、全空間に拡がるベクトル場の構造を知るという方法論である。更に、この動 4 面体の時間的な発展率（時間的な方向変化率と捻れ率の変化）導出も行った。これにより磁場幾何の 3 次元発展の記述も可能となる。

講演では、これらのフレームワークにより把握されるベクトル場の基本構造について概観し、その物理則による決定論について議論する。

R010-10
C 会場 ：11/4　PM2 （15:45-18:15）
16:50〜17:05

IGRF モデルおよび準 3 次元ポテンシャルソルバーを用いた M-I 結合系における EEJ 変動の構造解析

#伊集院　拓也 [1)], 吉川　顕正 [2)], 三好　勉信 [2)], 品川　裕之 [3)], 藤原　均 [4)], 陣　英克 [3)], 中溝　葵 [3)], 垰　千尋 [3)], 塩川和夫 [5)]
([1] 九大地球惑星科学専攻,[2] 九大地球惑星科学部門,[3] 情報通信研究機構,[4] 成蹊大・理工,[5] 名大宇地研

Analysis of EEJ structure in M-I coupling system using IGRF model and quasi-three-dimensional potential solver

#Takuya Ijuin[1)], Akimasa Yoshikawa[2)], Yasunobu Miyoshi[2)], Hiroyuki Shinagawa[3)], Hitoshi Fujiwara[4)], Hidekatsu Jin[3)], Aoi Nakamizo[3)], Chihiro Tao[3)], Kazuo Shiokawa[5)]
([1]Department of Earth and Planetary Sciences, Graduate School of Science, Kyushu University,[2]Department of Earth and Planetary Sciences, Faculty of Science, Kyushu University,[3]NICT,[4]Faculty of Science and Technology, Seikei University,[5]ISEE, Nagoya Univ.

What is happen at the magnetic equator in the Magnetosphere-Ionosphere coupling system? For example, Kikuchi [2000] suggested that penetration electric field extends from high latitude to equatorial region and Pedersen current connects polar regional current system and equatorial electrojet (EEJ). On the other hand, by two-dimensional potential solver, Yoshikawa et al. [2012] proposed Cowling channel model, in which auroral electrojet and EEJ are coupled as a result of occurrence of strong Hall polarization effect at the conductivity gradient region in sunlit / shadow region and magnetic equator, and associated of it, predicted the significant deformation of ionospheric potential. However, it does not achieve the reproduction of EEJ system in most previous studies about polar-equatorial coupling current system because they used two-dimensional current closure and simplified magnetic field model.

Therefore, we develop a quasi-three-dimensional electrostatic potential solver, and we are now reproducing three-dimensional current system at equatorial region in M-I coupling situation and analyzing to understand its excitation mechanism. We use IGRF model [e.g., Alken et al., 2021] as geomagnetic field and successfully reconstruct more realistic configuration of magnetic equator than earler M-I coupling simulations. In addition, we adopt the modified apex coordinates [Richmond, 1995] so that we can obtain three-dimensional distribution of any quantity in the ionosphere assuming the equipotentiality of magnetic field line although we calculate only two-dimensional second-ordered elliptic partial differential equation for electrostatic potential. This method is used in ionosphere-atmosphere coupling model [e.g., Takeda and Maeda, 1980; Kawano-Sasaki and Miyahara, 2008] and called quasi-three-dimensional model.

We report the analysis results of global ionospheric current. The results are reproduced with region-1 FAC based on Nakamizo et al. [2012] under the realistic three-dimensional conductivity from NRLMSIS-00 [Picone et al., 2002] and IRI-2016 [Biliza et al., 2017] for density and temperature of neutral and plasma species, respectively, and from Ieda [2020] for collision frequency. We analyze the calculation results of electrostatic potential and current density with the theory of polarization [Yoshikawa et al., 2013]. Finally, we find that EEJ in the M-I coupling system is made by primary Hall current from north-south component of penetration electric field. These results are quite different from the common theory that eastward penetration electric field is important for EEJ in M-I coupling. In this meeting, we will show the potential and current distributions from directly penetrate component.

磁気圏-電離圏（M-I）結合系において、磁気赤道ではどのような電流が流れるのだろうか。例えば、Kikuchi [2000] では、侵入電場が高緯度から赤道に幾何学的に広がり、極域電流系と赤道ジェット電流（EEJ）がペダーセン電流によって連結するモデルを提案している。一方、Yoshikawa et al. [2012] は、2 次元静電ポテンシャルソルバーにより、日照・日陰領域や磁気赤道領域での電気伝導度勾配領域で強いホール分極効果が発動した、オーロラジェット電流と EEJ が連結するカウリングチャンネルモデルを提唱し、それに伴う電離圏ポテンシャルの著しい変形を予想している。しかしながら、これらのモデルを含む過去の極域-磁気赤道域結合電流系の研究の大半では、2 次元的な電流系のクロージャーと簡略的な磁場モデルの採用により、特に高度方向の 3 次元電流形成が本質となる EEJ 系の再現は未だ実現していない。

本研究では、準 3 次元の静電ポテンシャルソルバーを開発し、M-I 結合系における磁気赤道の 3 次元電流系の再現と、その形成過程の理解に向けた解析調査を行っている。本ソルバーは、地球固有磁場として IGRF モデル [e.g., Alken et al., 2020] を実装し、従来の M-I 結合系の数値計算と比べて現実に近い磁気赤道の形状の再現に成功している。また、modified apex coordinates [Richmond, 1995] を適用し、磁力線の等電位性を仮定することにより、静電ポテンシャルの 2 次元 2 階楕円型偏微分方程式から、電離圏のあらゆる物理量の 3 次元分布を復元できる。この手法は電離圏-大気圏結合系のモデルで用いられており [e.g., Takeda and Maeda, 1980; Kawano-Sasaki and Miyahara, 2008]、準 3 次元モデルと呼ばれている。

今回は、全球電離圏結合電流系の解析結果について報告する。この結果は NRLMSIS-00 [Picone et al., 2002] と IRI-2016 [Biliza et al., 2017] から中性大気粒子と荷電粒子の密度と温度を計算し、Ieda [2020] の衝突周波数を組み合わせることにより求まった現実的な 3 次元電気伝導度の下、Nakamizo et al. [2012] をもとにした region-1 FAC の分布を入

力値として再現された。数値計算結果として得られた静電ポテンシャルと電流密度に対し、分極理論 [Yoshikawa et al., 2013] を用いた詳細解析を行った結果、極域から侵入する電場により励起される EEJ は南北方向の電場に対する 1 次のホール電流が主体であることがわかった。これは、東西方向の電場が侵入した結果 EEJ が生じるとされてきた、従来論とは大きく異なる描像である。本講演では、侵入電場の構造から順を追って各静電ポテンシャル成分や電流分布を紐解いていく。

R010-11
C 会場 ：11/4　PM2 （15:45-18:15）
17:05〜17:20

#張　天 [1)], 海老原　祐輔 [1)]
[(1] 京大生存圏

MHD simulations of responses of ionospheric currents and ground electric field variations under different solar wind conditions

#Tian Zhang[1)], Yusuke Ebihara[1)]
[(1]RISH, Kyoto Univ.

By performing a global magnetohydrodynamic (MHD) simulation, we investigated and calculated under different solar wind conditions (jump of velocity and density of solar wind), the response of ionospheric currents (Pedersen currents and Hall currents), the corresponding magnetic disturbance on the ground and the resultant geoelectric field variation by convolution method with an assumed ground conductivity. According to the results, we analyzed the change of geoelectric field as a function of magnetic latitude (MLAT) and magnetic local time (MLT), which may indicate the hazardous area where E (geoelectric field) becomes large in response to jump of Vsw (velocity of solar wind) and/or Nsw (density of solar wind). This also helps us to better understand the generation of large geomagnetically induced currents. At last, we compared the simulation results of dB (geomagnetic disturbance) with that of the known Quebec blackout in 1989, and discuss the cause of the large GIC that flowed in the power grid in Canada.

R010-12
C 会場 ：11/4　PM2 （15:45-18:15）
17:20〜17:40

#小川　泰信 [1)], 宮岡　宏 [1)], 野澤　悟徳 [2)], 橋本　大志 [1)], 大山　伸一郎 [3)], 西村　耕司 [1)], 津田　卓雄 [4)], 藤原　均 [5)], 堤　雅基 [1)], 田中　良昌 [1)], 西山　尚典 [1)], 吹澤　瑞貴 [1)], 中村　卓司 [1)], 藤井　良一 [6)],Heinselman　Craig[7)]
([1] 極地研,[2] 名大・宇地研,[3] 名大 ISEE,[4] 電気通信大学,[5] 成蹊大学,[6] 情報・システム研究機構,[7]EISCAT 科学協会

EISCAT_3D and Japan's Activities

#Yasunobu Ogawa[1)], Hiroshi Miyaoka[1)], Satonori Nozawa[2)], Taishi Hashimoto[1)], Shin ichiro Oyama[3)], Koji Nishimura[1)], Takuo Tsuda[4)], Hitoshi Fujiwara[5)], Masaki Tsutsumi[1)], Yoshimasa Tanaka[1)], Takanori Nishiyama[1)], Mizuki Fukizawa[1)], Takuji Nakamura[1)], Ryoichi Fujii[6)], Craig Heinselman[7)]
([1]NIPR,[2]ISEE, Nagoya Univ.,[3]ISEE, Nagoya Univ.,[4]The University of Electro-Communications,[5]Seikei University,[6]ROIS,[7]EISCAT Scientific Association

The European Incoherent Scatter (EISCAT) Scientific Association started construction of the first stage of the EISCAT_3D radar in 2017 under international collaboration. The EISCAT_3D radar is expected to be operational in 2023. At the first stage, a core site with a transmission power of about 4~5 MW and two receive-only remote sites will be operated. The ground preparation for the three sites is in progress, and each radar unit is installed at the sites in 2022. The EISCAT_3D radar is expected to be utilized for a variety of science cases, including study on energy and mass transport from the solar wind and magnetosphere to the ionosphere and atmosphere. The results and real-time data distribution will contribute to space climate research and space weather forecasting.

The National Institute of Polar Research (NIPR) had been contributing to the EISCAT_3D construction by supplying radar transmitter power amplifiers (SSPAs) in collaboration with the EISCAT scientific association and ISEE Nagoya University. The high energy-efficient SSPAs have been used for engineering verification tests at the EISCAT Tromsoe and Kiruna sites since 2016. In February 2020, NIPR has concluded an MoU with EISCAT to supply in-kind Subarray Transmitter Units which are selected for the first stage by the EISCAT Headquarters through the international tendering process. After these contributions to the EISCAT_3D construction, NIPR establishes the Advanced Radar Research Promotion Center in April 2022 to promote joint usage and collaborative research of the EISCAT_3D radar.

In this paper we present the status of the EISCAT_3D implementation and discuss the prospects for Japan's EISCAT_3D activities.

R010-13
C 会場 ：11/4　 PM2 （15:45-18:15）
17:40〜17:55

SuperDARN 北海道-陸別第一・第二レーダーで観測された SAPS 構造の緯度分布について

#西谷　望 [1)], 堀　智昭 [1)]
(1 名大 ISEE

On the latitudinal distribution of the SAPS structure observed by the SuperDARN Hokkaido Pair of radars

#Nozomu Nishitani[1)], Tomoaki Hori[1)]
([1]ISEE, Nagoya Univ.

The latitudinal distribution of subauroral polarization streams (SAPS) is discussed based on the over 15 years of observation achieved by the SuperDARN Hokkaido Pair of radars. Previous statistical studies showed that the latitudinal position of the SAPS structure could be predicted on average as a function of magnetic local time and Dst geomagnetic index. In this presentation, two examples (8 Sep 2017 and 4 Nov 2021 events) are compared in detail with each other, showing similar Dst index values and taking place at similar magnetic local times but located at significantly different geomagnetic latitudes. Some initial results of the statistical analysis are also presented.

SuperDARN 北海道-陸別第一・第二レーダーは地球上の高・中緯度域に分布する計 30 基以上の SuperDARN レーダーの中で最も低い地磁気緯度に位置している。これの地理的優位性を活用して、過去には SAPS 構造の緯度分布の地磁気活動度分布について複数の統計的研究がおこなわれてきた (e.g., Kataoka et al., 2008; Nagano et al., 2015)。これらの研究では、磁気地方時、Dst 指数と SAPS の磁気緯度との間に統計的に関連性があることが示されている。ただし当時使用したデータベースでは 1 太陽周期を網羅することができず、データ数も十分なものとは言えなかった。

2006 年 11 月に SuperDARN 北海道-陸別第一レーダーが稼働を開始してから 15 年以上が経過し、太陽活動についても 1 周期分をカバーできるデータベースが蓄積されており、より詳細な関連性の議論が可能となっている。例として 2017 年 9 月の地磁気嵐と 2021 年 11 月の地磁気嵐における SAPS の緯度分布を比較すると、Dst の負のピークはそれぞれ-122nT と-105nT、SAPS 構造の観測された磁気地方時は約 23 時と約 22 時のようにほぼ条件は同じであるが、視線方向速度が 400m/s 以上の SAPS 構造の地磁気緯度は 49 度と 52 度と大きく異なっていた。この違いを起こす要因として、IMF・太陽風の履歴、サブストームの発生状況等が考えられるが、詳細な議論は講演で示す予定である。

R010-14
C 会場 ：11/4　PM2 （15:45-18:15）
17:55〜18:10

サブストーム時の CW 発達に伴う中緯度領域/地上磁場・電場観応答の考察

#林　萌英 [1)], 吉川　顕正 [2,3)], 藤本　晶子 [4)],Ohtani　Shinichi[5)]
([1] 九州大学理学府地球惑星科学専攻,[2] 九州大学理学研究院 地球惑星科学部門,[3] 国際宇宙惑星環境研究センター,[4] 九州工業大学,[5] ジョンズホプキンス大学応用物理研究所

Investigation of the response of magnetic and electric fields in mid-latitude to the development of CW during substorms

#Moe Hayashi[1)], Akimasa Yoshikawa[2,3)], Akiko Fujimoto[4)], Shinichi Ohtani[5)]
([1]Graduate School of Earth and Planetary Sciences, Kyushu University,[2]Department of Earth and Planetary Sciences, Kyushu University,[3]Research Center for Space and Planetary Environmental Science,[4]Kyushu Institute of Technology,[5]Johns Hopkins University Applied Physics Laboratory

The purpose of this study is to comprehensively understand the evolution of global 3D current system from polar to equatorial ionosphere during substorms.

There are two types of current systems in the polar ionosphere: the R1-current linked to the magnetospheric convection system, and the R2-current linked to the pressure gradient in the inner magnetosphere [Iijima and Potemra, 1976, 1978]. In addition to these currents, when a substorm onset is occurred by a strong plasma injection, a current wedge (CW) is generated by the plasma vorticities at the edge of the plasma flow. It has the same current polarities as the R1-current system.

Magnetic field variations generated by field-aligned currents (FAC) associated with CW development are significant in the nightside mid- and low-latitude, and these variations was modeled by McPherron et al. [1973]. We capture the development of CW current systems during substorm by using MAGDAS and SuperMag magnetic field data, and by comparing them with the electric field data from the FM-CW installed at Kyushu University in Paratunka, Russia, we are analyzing the electromagnetic dynamic responses in the mid- and low-latitude regions.

By comparative analysis of the ionospheric electric and geomagnetic field on isolated substorms that occurred from September 21, 2006, to December 31, 2010, we found that there are three patterns of electric field variations at mid-latitudes near the current wedge. The amplitude of the electric field variation is correlated with the westward auroral electrojets strength. The direction of the electric field cannot be explained by the electric field associated with the CW current system, however, it reflects the electric field caused by the Hall polarization effect due to the ionospheric current induced by CW (simulated by Yoshikawa et al. [2013]). In this presentation, we report the results of a more detailed analysis of the characteristics of the electric field amplitude associated with the development of the CW structure and the difference from the inner and outer boundaries of the CW.

本研究の目的は、サブストーム時の極域から赤道域までのグローバルな 3 次元電流システムの進化を地上磁場観測と FM-CW 電場観測に基づき包括的に理解することにある。

極域電離圏の電流システムには、磁気圏対流系の消長と連動する R1-電流と、内部磁気圏の圧力勾配領域の消長と連動する R2-電流が存在する [Iijima and Potemra, 1976, 1978]。これに加えて、サブストームのオンセット時には、R 1 電流系と同様の電流クロージャーを形成するカレント・ウェッジ（CW）電流系が発達することが知られている。

CW の成長に伴う沿磁力線電流が作る磁場変動は、夜側の中低緯度領域で顕著であり、その発展の様子は McPherron et al.(1973) によってモデル化されている。我々は、MAGDAS および SuperMag の地上磁場データを用いて、オーロラサブストーム時の CW 電流系の成長を捉え、九州大学がロシア・パラツンカに設置する FM-CW 電離圏観測機器の電場データと比較することにより、中低緯度領域の電磁力学的応答特性の解析を進めている。

2006 年 9 月 21 日〜2010 年 12 月 31 日に発生した孤立型サブストームの電離圏電場と地磁気を比較解析した結果、CW 付近の中緯度の電場変動に 3 つのパターンがあることを発見した。この電場変動の振幅は西向きオーロラエレクトロジェット電流の強度と相関関係があり、その方向に関しては、CW 電流系に伴う電場だけでは説明出来ず、Yoshikawa et al.[2013] により示された CW に伴い励起される電離層電流による Hall 分極効果によって生じる電場特性を反映していることが明らかになった。本発表では、CW の構造成長や、CW の内・外境界からの経度差に伴う電場振幅の分布特性をより詳細に解析した結果を報告する。

R010-15
C 会場 ：11/5　AM1 （9:00-10:30）
09:00〜09:15

#斎藤　享 [1)], 吉原　貴之 [2)], 高橋　透 [3)]
([1] 電子航法研,[2] 電子航法研,[3] 電子航法研

Impacts on GNSS by ionospheric irregularities observed over Japan on 15 January 2022

#Susumu Saito[1)], Takayuki Yoshihara[2)], Toru Takahashi[3)]
([1]ENRI, MPAT,[2]ENRI, MPAT,[3]ENRI, MPAT

On 15 January 2022, various ionospheric disturbances were observed over Japan. Traveling ionospheric disturbances (TIDs) which were shown to be associated with the volcanic eruption of Hunga Tonga-Hunga Ha'apai, Tonga (Saito, EPS, 2022). Following the TIDs, another types of ionospheric disturbances accompanying enhanced small-scale irregularities represented by the rate of the total electron content (TEC) index (ROTI) were observed at several locations over Japan at geographic latitudes as high as 38N (33.8 in the magnetic latitude). The characteristics of the irregularities appeared to be similar to those associated with the storm-enhanced density (SED) or storm-induced plasma stream (SIPS) observed in the geomagnetic storms (Saito et al., JPGU, 2022). They were unusual ionospheric disturbances, because the geomagnetic activities were not so high as to excite SED or SIPS events. It was also unusual to have strong irregularities at such higher latitudes. At the same time, ionospheric irregularities were also observed at the low latitude part of Japan. In this study, impacts of these unusual ionospheric irregularities on applications of Global Navigation Satellite System (GNSS).

We used GNSS observation data from GNSS receivers of the GNSS Earth Observation Network (GNSS) operated by the Geospatial Information Authority of Japan (GIS). ROTI maps generated by the data from GEONET is used to identify the spatial and temporal variation of the irregularity structures. Closely separated GNSS station pairs are used to estimate the spatial variation of the ionospheric TEC which is equivalent to the propagation delay of the GNSS signals.

GNSS scintillation receivers at Ishigaki (24.3N, 124.2E, 19.6 Magnetic Latitude) are used to observe the small-scale irregularities. A set of closely separated GNSS receivers with mutual distances of 0.1-2.2 km located at the New Ishigaki Airport is used to evaluate the impacts of the ionospheric irregularities on the GNSS ground-based augmentation system (GBAS) which is the aeronautical navigation system to guide aircraft for approach and landing. There were 13 and 10 GPS/Galileo/QZSS satellites transmitting at L1 and L5 bands, respectively and 9 and 9 satellites for L1 and L5, respectively experienced the S4 index stronger than 0.25. However, the spatial TEC variations were not so much as those typically associated with the plasma bubbles. Indeed, the irregularities were associated with TEC depletions embedded in regions of TEC enhancement, which is different from the typical plasma bubbles.

References:

Saito, S. (2022), Ionospheric disturbances observed over Japan following the eruption of Hunga Tonga-Hunga Ha'apai on 15 January 2022, Earth, Planets and Space, https://doi.org/10.1186/s40623-022-01619-0.

Saito, S., Yoshihara, T., Takahashi, T. (2022), Ionospheric irregularities and scintillations during the geomagnetic storm on 15 January 2022, JPGU2022.

R010-16
C 会場 ：11/5　AM1 （9:00-10:30）
09:15〜09:30

#中村　真帆 [1)], 斎藤　享 [1)], 吉原　貴之 [1)],Le huy Minh[2)]
([1 電子航法研,([22 Institute of Geophysics, Vietnam Academy of Science and Technology（IGP-VAST), Vietnam

Preliminary results on the ionospheric delay gradient as a threat to GBAS in the equatorial ionization anomaly crest region

#Maho Nakamura[1)], Susumu Saito[1)], Takayuki Yoshihara[1)], Minh Le huy[2)]
([1ENRI, MPAT,([22 Institute of Geophysics, Vietnam Academy of Science and Technology（IGP-VAST), Vietnam

In recent years, Ground-based augmentation system (GBAS), which is an aeronautical navigation system for precision approach and landing based on the single-frequency differential GNSS technique, has been put into practical use, and its installation is expected to expand in the low magnetic latitude region including Japan. Although GBAS provides accurate position solutions by broadcasting ionospheric delay corrections based on observations by ground reference receivers, steep and narrow ionospheric gradients may be undetectable and poses a threat to the system.

It is known that the steep ionospheric gradient caused mainly by the equatorial plasma bubbles (EPBs) in the low magnetic latitude region. Previous studies have also suggested that such a steep spatial gradient is generated by EPB. Previous studies also confirmed that the generation of such steep spatial gradients is consistent with the generation characteristics of EPB.

International Civil Aviation Organization (ICAO) has conducted data collection and analysis, and characterized the ionospheric delay gradient variation, which is called an ionospheric threat model for GBAS in the Asia-Pacific (APAC) region [1]. It treats all the equatorial and low latitude regions together. However, due to different geometries between the ground station, GNSS satellites, and the ionosphere, the ionospheric threat model could be different within the region. Especially, the equatorial ionization anomaly (EIA) crests and EPBs develop into the EIA crests would result in spatial variations of the characteristics of the ionospheric gradient observed at a certain location on the ground. Therefore, the ICAO APAC GBAS ionospheric threat model could be a conservative one, and could be optimized for each location to reasonably reduce the conservativeness. Therefore, more observations in different locations within the equatorial and low magnetic latitude regions are necessary. Therefore, In order to understand the variation of the GBAS ionospheric threat model within the magnetic equatorial and low latitude region, ENRI has deployed networks for a steep ionospheric gradient observation from 2021 in Vietnam, and from 2022 in Indonesia, which is located in the EIA crest regions.

In this study, we will show the initial results of the ionospheric steep gradient analysis in Vietnam.

References

[1] Saito, S. et al. (2017), Ionospheric delay gradient model for GBAS in the Asia-Pacific region, GPS Solutions, 21:1937-1947, doi:10.1007/s10291-017-0662-1.

R010-17
C 会場 ：11/5　AM1 （9:00-10:30）
09:30〜09:45

リアルタイム GAIA を用いたプラズマバブル発生予測システムの開発

#品川　裕之 [1)], 垰　千尋 [1)], 陣　英克 [1)], 三好　勉信 [2)], 藤原　均 [3)]
([1] 情報通信研究機構,[2] 九大・理・地球惑星,[3] 成蹊大・理工

Development of a prediction system of plasma bubble occurrence using real-time GAIA

#Hiroyuki Shinagawa[1)], Chihiro Tao[1)], Hidekatsu Jin[1)], Yasunobu Miyoshi[2)], Hitoshi Fujiwara[3)]
([1]NICT,[2]Dept. Earth & Planetary Sci, Kyushu Univ.,[3]Faculty of Science and Technology, Seikei University

Prediction of ionospheric disturbances is one of the most important issues in space weather forecast. In particular, the prediction of plasma bubbles becomes more and more important because plasma bubbles have significant influences on social infrastructure such as positioning using GPS and communication systems. Prediction of plasma bubbles requires a real-time numerical model which is able to reproduce and predict ionospheric conditions as well as real-time ionospheric observations in the low-latitude region. We have been developing an atmosphere-ionosphere coupled model GAIA, which includes the whole atmosphere and ionosphere self-consistently. Although present version of GAIA does not have enough spatial resolution to directly reproduce plasma babbles, it may be possible to deduce the occurrence of plasma bubbles from ionospheric conditions in GAIA. In our previous study, we found that the linear growth rate of the ionospheric Rayleigh-Taylor instability (RTI) obtained from GAIA data can be used as an index of plasma bubble occurrence. The result indicated that larger RTI growth rate tends to correspond to larger probability of plasma bubble occurrence [Shinagawa et al., 2018], suggesting the possibility of numerical prediction of plasma bubble occurrence. However, it was not certain whether or not it is possible to predict the occurrence of plasma bubbles one or two days in advance with enough accuracy. Recently, we have started to operate a real-time GAIA simulation at NICT, which is able to provide ionospheric parameters about two days in advance [Tao et al., 2020]. Using the real-time GAIA, it is technically possible to predict the plasma bubble occurrence in about two days in advance. We are currently developing a plasma bubble prediction system at NICT using the real-time GAIA. We will report the current status of the system, and discuss future prospects and problems.

References

Shinagawa, H., Y. Miyoshi, H. Jin, H. Fujiwara, T. Yokoyama, and Y. Otsuka (2018). Daily and seasonal variations in the linear growth rate of the Rayleigh-Taylor instability in the ionosphere obtained with GAIA, Progress in Earth and Planetary Science, 5:16. https://doi.org/10.1186/s40645-018-0175-8

Tao, C., H. Jin, Y. Miyoshi, H. Shinagawa, H. Fujiwara, M. Nishioka, and M. Ishii (2020). numerical forecast of the upper atmosphere and ionosphere using GAIA. Earth Planets Space, 72:178. https://doi.org/10.1186/s40623-020-01307-x

電離圏擾乱の予測は宇宙天気予報における最重要課題の一つである。特に電離圏プラズマバブルは測位や通信等の社会インフラに大きな影響を及ぼす可能性があることから、近年その予測の重要性は急速に高まりつつある。プラズマバブルの予測を行うためには低緯度地域でのリアルタイム電離圏観測とともに、リアルタイムで電離圏の現況把握や予測を行える数値モデルが必要である。我々は下層大気から熱圏・電離圏領域までを含む全大気圏-電離圏結合モデル GAIA を開発してきた。現行版の GAIA は分解能がまだ荒いため、直接プラズマバブルを再現することはできないが、GAIA 中の電離圏の状態からプラズマバブルの発生しやすさを推定できる可能性がある。これまでの研究で我々は、GAIA で計算された電離圏のレイリー・テイラー不安定性の線形成長率が大きい日ほどプラズマバブルの発生確率が高いことを見出した [Shinagawa et al., 2018]。この結果はプラズマバブル発生の数値予測の可能性を示唆した点で重要な一歩ではあるが、実際に 1 日〜数日程度先のプラズマバブルの発生予測が十分な精度で行えるかどうかは明らかではない。我々はリアルタイム GAIA を開発し、情報通信研究機構 (NICT) において約 2 日先までの電離圏の予測値を与えるシステムを稼働している [Tao et al., 2020]。このシステムを用いれば、レイリー・テイラー不安定性の線形成長率を求める方法により約 2 日先までのプラズマバブル発生確率を求めることが技術的には可能である。現在我々はリアルタイム GAIA を用いたプラズマバブル発生予測システムの開発を進めている。本講演では、現状の報告と今後の展望、問題点等について議論する。

参考文献

Shinagawa, H., Y. Miyoshi, H. Jin, H. Fujiwara, T. Yokoyama, and Y. Otsuka (2018), Daily and seasonal variations in the linear growth rate of the Rayleigh-Taylor instability in the ionosphere obtained with GAIA, Progress in Earth and Planetary Science, 5:16. https://doi.org/10.1186/s40645-018-0175-8

Tao, C., H. Jin, Y. Miyoshi, H. Shinagawa, H. Fujiwara, M. Nishioka, and M. Ishii (2020). numerical forecast of the upper atmosphere and ionosphere using GAIA. Earth Planets Space, 72:178. https://doi.org/10.1186/s40623-020-01307-x

R010-18
C 会場 ：11/5　AM1 （9:00-10:30）
09:45〜10:00

#北島　慎之典 [1)], 渡邉　恭子 [1)], 西本　将平 [1)], 陣　英克 [2)], 垰　千尋 [2)], 西岡　未知 [2)]
([1] 防衛大,[2] 情報通信研究機構,[3] 情報通信研究機構

Scale estimation of the Dellinger phenomenon using the GAIA model

#Shinnosuke Kitajima[1)], Kyoko Watanabe[1)], Shohei Nishimoto[1)], Hidekatsu Jin[2)], Chihiro Tao[2)], Michi Nishioka[2)]
([1]NDA,[2]NICT,[3]NICT

The sudden increase in X-ray to extreme ultraviolet (EUV) emissions of solar flares promote ionization in the ionosphere and it can cause a rapid variation in electron density. The communication failure caused by the absorption of the radio waves (HF; High Frequency), due to the variations in electron density in the ionospheric D region (60-90 km) is called the Dellinger phenomenon (Dellinger 1937). The occurrence of the Dellinger phenomenon can be known from the value of the minimum reflection frequency (fmin) observed by the vertical incident ionosonde. It is known that the fmin value fluctuation depends on the peak X-ray intensity of flare and the solar zenith angle (e.g., Tao et al., 2020), and the current estimation of Dellinger phenomenon is based only on solar X-ray observations. However, this relationship has large fluctuations and there are many cases in which the fmin value is not proportional to the X-ray peak flux. Thus, it is necessary to consider not only X-rays but also other flare emission wavelengths that affect the electron density in the lower ionosphere. The main candidate for this non-X-ray emission affecting the Dellinger phenomenon is EUV emissions.

First we investigated the relationship between the observed X-ray and EUV emissions during flares and the fmin values. In this study, we analyzed 38 solar flare events of M3 class or larger observed during daytime in Japan (9:00-18:00 JST) between May 2010 and May 2014. We used the GOES/X-ray Sensor (XRS) for X-ray data, the GOES/Extreme Ultraviolet Sensor (EUVS) and the Solar Dynamics Observatory (SDO)/EUV Variability Experiment (EVE) were used for EUV data. The fmin values were obtained from ionograms which are provided by the National Institute of Information and Communications Technology (NICT) in Wakkanai, Kokubunji, Yamagawa and Okinawa.

Comparing these X-ray and EUV emissions with fmin values, we found that the Lyman-alpha emission from the GOES/EUVS-E does not correlate with fmin values. On the other hand, X-ray (0.1-0.8 nm) and EUV (11-14 nm) emissions correlate with fmin values, with correlation coefficients of 0.74 and 0.76, respectively.

Next, we used the Ground-to-Topside Model of Atmosphere and Ionosphere for Aeronomy (GAIA) provided by NICT, a physical model of the Earth's atmosphere, to calculate the ionospheric effects of solar flare emission and compare them with the fmin value. Since GAIA provides the altitude profile of the electron density change at each wavelength of the solar flare spectrum.

We analyzed the X1.7-class flare event on May 13, 2013, in detail. The results show that at an altitude of around 100 km, the ion production rate from X-rays is about 6 orders of magnitude larger than that of 11-14 nm EUV emission, indicating that X-rays are the main source of ion density fluctuations at this altitude. On the other hand, the ion production rates in the E and F regions around 100-150 and 150-400 km altitude are 1 or 2 orders of magnitude larger for the 11- 14 nm EUV emission than for X-rays, indicating that the 11-14 nm EUV emission is the main cause of the ion density fluctuations at the E and F regions.

The absorption rate of HF radio was ˜90-95 % around 100 km altitude and ˜5- 10 % in the E region (100-150 km altitude).

The current GAIA model is not able to calculate accurately below about 100 km altitude, but Dellinger phenomenon occurs in the D region below about 100 km altitude, and the fmin value is also measured in the D region. Therefore, in this study, we tried to estimate the electron density at altitudes below 100 km by using the electron distribution at 100 km altitude calculated by GAIA as an initial value. In this paper, we will discuss the estimated electron density in the ionosphere D region and their relationship between the Dellinger phenomenon.

R010-19
C 会場 ：11/5　AM1 （9:00-10:30）
10:00〜10:15

#北村　健太郎 [1,5], 藤本　晶子 [1,5], 寺本　万里子 [2,5], 吉川　顕正 [3,4], 阿部　修司 [4]
([1] 九州工大/工,[2] 九州工大/情報工,[3] 九大/理学研究院,[4] 九大・i-SPES,[5] 九州工大/LaSEINE

Eastward Magnetic Variations in the Equatorial Latitude Associated with the IH-FAC Observed on the Ground and LEO

#Kentarou Kitamura[1,5], Akiko Fujimoto[1,5], Mariko Teramoto[2,5], Akimasa Yoshikawa[3,4], Shuji Abe[4]
([1]Kyutech,[2]Kyutech,[3]Kyushu Univ.,[4]i-SPES, Kyushu Univ.,[5]Kyutech/LaSEINE

The Inter-Hemispheric Field Aligned Currents (IHFAC) are considered to be produced by the north/south asymmetry of the potential in the ionosphere. Maeda (1974) and Fukushima (1979, 1991) theoretically predict the existence of the IHFAC, that is, the IHFAC flows from winter hemisphere to summer hemisphere at the noon and evening sectors and summer to winter hemisphere at the morning sector. On the other hand, several ground-based (Yamazaki et al., 2009, Owolabi et al., 2018) and satellite (Yamashita and Iyemori, 2002, and Park et al., 2002, 2020) observations have been demonstrated by many investigators, which revealed the morphology of the FAC.

Recently, Ranasinghe et al. (2021) pointed out that the eastward magnetic variations at DAV station (Geographical latitude 7 deg., Geographical longitude 124.5, Geomagnetic latitude -2.22 deg, Geomagnetic longitude 197.9 deg, Dip latitude -0.24 deg) shows the positive variations (equivalent to the northward current) at the evening sector during the northern summer. Their results suggested that the seasonal and local-time dependence of the direction of IHFAC shows inconsistency with the prediction by Fukushima (1979).

In this study, the data from the Vector Magnetic Field (VMF) onboard the Swarm satellites were analyzed to compare the magnetic variations associated with the IHFAC with the ground magnetic observations. The magnetic data of the VMF were chosen in the condition that the position of the satellites is within -5 to 5 degrees in latitude and within 115 to 135 degrees in longitude. These criteria are almost equivalent to the location of DAV ground station.

The result indicates that the eastward component of the VMF data shows the clear seasonal and local-time dependences associated with the IHFACs. During the northern summer, the magnetic variations in the eastward variations are strongly negative in the noon sector which indicates the northward current is predominant in the noon. On the other hand, the local time in the range between 12 and 18 LT, the eastward component of the magnetic variations shows obvious seasonal dependence of the IHFAC. The intensification of southward IHFAC appears in the confined local-time around 17 LT in July, then range of LT for southward IHFAC increases with increasing of month, which shows maximum local-time range of 12-17 LT for southward currents in December. These characteristics could not be interpreted by the conventional understanding of IHFAC and suggests that the ionospheric conductivities in the evening terminator might play an important role in the generation of the IHFAC.

R010-20
C 会場 ：11/5　AM1 （9:00-10:30）
10:15〜10:30

#ぎるぎす　きろろす[1)], 羽田　亨[2)], 吉川　顕正[3)], 松清　修一[4)], ルメール　ジョゼフ[5,6)], ピエラル　ヴィヴィアン[6,7)], スザン　サムウェル[8)]
([1]九州大学 国際宇宙惑星環境研究センター,[2]九大総理工,[3]九大/理学研究院,[4]九大・総理工,[5]Faculty of Science, Catholic University of Louvain (UCL), BELGIUM,[6]Royal Belgian Institute for Space Aeronomy (BIRA-IASB), BELGIUM,[7]Center for Space Radiations, Catholic University of Louvain (UCL), BELGIUM,[8]National Research Institute of Astronomy and Geophysics (NRIAG), EGYPT

How do the geomagnetic storms affect the LEO proton flux distribution during Solar Energetic Particle events?

#Kirolosse Girgis[1)], Tohru Hada[2)], Akimasa Yoshikawa[3)], Shuichi Matsukiyo[4)], Joseph Lemaire[5,6)], Viviane Pierrard[6,7)], Samwel Susan[8)]
([1]i-SPES, Kyushu University,[2]Kyushu University,[3]Kyushu University,[4]Kyushu University,[5]Faculty of Science, Catholic University of Louvain (UCL), BELGIUM,[6]Royal Belgian Institute for Space Aeronomy (BIRA-IASB), BELGIUM,[7]Center for Space Radiations, Catholic University of Louvain (UCL), BELGIUM,[8]National Research Institute of Astronomy and Geophysics (NRIAG), EGYPT

The precipitation of the Solar Energetic Particles (SEP) into the trapping region of the Earth's inner magnetic field was reported by several satellite observations. When the SEP events coincide with geomagnetic storms, the particle precipitation becomes deeper and can access to lower latitude regions. This phenomenon is considered as a dangerous situation for most of the LEO missions, especially the high-inclined orbit missions.

In order to examine how the geomagnetic storms can affect the LEO proton flux distribution during SEP events, we have developed a three-dimensional relativistic test particle simulation code to compute the 70-180 MeV solar proton full trajectories in the inner radiation belt of L-shell range (1 <L <3). We have selected three different Dst index values: -7, -150 and -210 nT, to define quiet time, strong and intense geomagnetic storm conditions and to generate the corresponding geomagnetic field by adopting IGRF model (v12) and Tsyganenko model (T01).

We found that, as long as the magnetic storm was intensified, the proton flux became more prominent at the higher latitude zones and more expanding toward lower latitude range. In addition, the proton flux distribution in the lower latitude zones which includes the South Atlantic Anomaly (SAA), became more flattened as the Dst index was decreased. Finally, the assessment of the corresponding radiation environment showed that a Polar LEO mission could be subjected to 20% excess Single Event Upset (SEU) rates during intense geomagnetic storm.

R010-21
C 会場 ：11/5　AM2 （10:45-12:30）
10:45〜11:00

磁気圏 MHD シミュレーションによる地磁気誘導電流（GIC）予測の検討 3

#亘　慎一 [1)], 中溝　葵 [1)], 海老原　祐輔 [2)]
[(1] 情報通信研究機構,[(2] 京大生存圏

Estimation of geomagnetically induced current (GIC) using the global MHD simulation of the magnetosphere 3

#Shinichi Watari[1)], Aoi Nakamizo[1)], Yusuke Ebihara[2)]
[(1]NICT,[(2]RISH, Kyoto Univ.

We have studied the estimation of geomagnetically induced current (GIC) using the results of the global MHD simulation of the magnetosphere, which is computed in real time in the National Institute of Information and Communications Technology (NICT). For the estimation of GIC, the following steps are required: (1) calculation of magnetic variation from the result of the magnetospheric simulation, (2) calculation of electric filed variation from the geomagnetic variation, and (3) calculation of GIC from the electric field variation.

According to (1), we analyzed relatively long-term data and showed that the high-latitude geomagnetic variation calculated from the result of the magnetospheric simulation is highly correlated with observation data. On middle and low latitudes geomagnetic variation, the correlation between SYM-H and the calculated one is not so good while there is a high correlation between the cross polar cap potential (CPCP) calculated form the magnetospheric simulation and PC-index. According to (2), we showed that electric field variation can be calculated from geomagnetic variations in the time domain using convolution integration. According to (3), we showed that the GIC observation data can be explained by applying the electric filed observed at Kakioka as a uniform electric field into the simplified transmission line model.

We reexamined the calculation of geomagnetic variation at middle and low latitudes by comparison with observed data and made the calculation of electric field from geomagnetic variation in the frequency domain. We will report on them.

リアルタイム計算を行っている NICT のグローバル磁気圏 MHD シミュレーションの結果を用いて地磁気誘導電流（GIC, Geomagnetically Induced Current）を予測するための検討を行っている。GIC の予測を行うためには、（1）磁気圏シミュレーションの結果から地磁気変動の計算、（2）地磁気変動から電場変動の計算、（3）電場変動から GIC の計算という手順が必要となる。
これまで、（1）について比較的長期間の観測データとの比較検討を行い、高緯度の地磁気変動について磁気圏シミュレーションから算出した地上の地磁気変動と観測データとの相関が高いことを示した。一方、磁気圏シミュレーションから算出した極間電位（CPCP, cross polar cap potential）と PC-index とは相関が高いが、CPCP を使って算出した SYM-H についてあまり相関がよくないという課題があった。（2）については、畳み込み積分を使用した時間領域での計算で地磁気データから電場データの計算ができることを示した。（3）については、柿岡で観測された電場を簡略化した送電線モデルに一様な電場として与えることにより GIC の観測データを説明できることを示した。
今回は、観測データとの比較により中低緯度の地磁気変動の計算について再検討を行った。また、地磁気変動から電場変動の計算について周波数領域での計算について検討を行った。本発表では、これらの結果について報告する。

R010-22
C 会場 ：11/5　AM2 （10:45-12:30）
11:00〜11:15

#中村　紗都子 [1)], 海老原　祐輔 [2)], 亘　慎一 [3)], 後藤　忠徳 [4)]
([1]IAR&ISEE,([2] 京大生存圏,([3] 情報通信研究機構,([4] 兵庫県立大学

Drastic time variations of transfer function of geomagnetically induced current (GIC) in Japan

#Satoko Nakamura[1)], Yusuke Ebihara[2)], Shinichi Watari[3)], Tadanori Goto[4)]
([1]IAR&ISEE,([2]RISH, Kyoto Univ.,([3]NICT,([4]Univ. Hyogo,

Geomagnetically induced currents (GICs) flow in power grid in response to geomagnetic field variations. Because of the potential threat of power outage, GIC is regarded as one of the important aspects of space weather. We calculated the transfer function in frequency domain that describes a linear relationship between the GICs measured at 3 substations in Japan and the geomagnetic field measured at the Kakioka observatory. The transfer function is found to show a significant time variation. For the periods at 2 to10 minutes, the amplitude of the transfer function in night time is about 1 order of magnitudes larger than in day time. The day-night difference reduces for the periods $>$100 minutes. In addition, the amplitude of the transfer function tends to increase with local rainfall amount. These regular and irregular variations may be explained in terms of earthing resistivity depending on local weather conditions. The resistivity of the non-frozen soil decreases by about 40% when the temperature increases from 15 to 35 degrees, resulting in the reduction of the earthing resistivity. Rainwater permeating into the soil also results in reduction of the earthing resistivity. Reduction of the earthing conductivity gives rise to magnification of the GICs. These results imply that a weather condition strongly affects the magnitude of GIC in Japan and challenge the conventional wisdom that the transfer function is almost steady in this time scale.

R010-23
C 会場 ：11/5　AM2 （10:45-12:30）
11:15〜11:30

大振幅 SC の特性 (2)

#荒木　徹 [1)]
(1 京大理

Characteristics of large amplitude SC (2)

#Tohru Araki[1)]
(1Formerly, Kyoto Universiy

When a solar wind shock strongly compresses the magnetosphere to produce a geomagnetic sudden commencement (SC), the magnetopause may enter the inside of the geosynchronous orbit. At this time, the dayside size of the magnetosphere will be reduced to about half, and the resulted large amplitude SC is thought to exhibit properties different from those of medium- and small-amplitude SCs. Analysis of this large-amplitude SC will reveal magnetospheric responses to strong compression that cannot be known from ordinary SCs. Based on this expectation, we are investigating large-amplitude SCs.

According to the list of SC at KAKIOKA since 1924, the H component amplitude of most SCs is in the range of 10-30nT. SCs of 50 nT or larger are less than 5%, and SCs larger than 100 nT are about 1%. Only 3 SCs show amplitude larger than 200 nT.

Here we report two characteristics of large amplitude SCs.

(1) Some large-amplitude SCs are accompanied by a short large pulse at the beginning. For example, an SC on March 24, 1991 which is third largest SC since 1868, was started with a global large and short pulse (202 nT amplitude, 90 sec pulse width at KAKIOKA. Large pulses appear at the tip of the largest 1940.3.24 SC (more than 273nT at KAKIOKA) and the second largest 1960.11.13 SC (220 nT).

When a stepwise compression propagates in the day side magnetosphere toward the earth, a westward electric field is created along the wave front of increasing magnetic field, and it is projected onto the polar ionosphere to create a PI (Preliminary Impulse) current system. In the case of a short pulse propagation, an eastward electric field is produced along the wave front of the decreasing magnetic field so that the projected polar electric field changes from westward to eastward, and two opposite sense PI current systems appear successively. The validity of this idea has been confirmed by a model calculation in the case of 1991.3.24SC.

(2) We examined LT variation of amplitude of SCs at KAKIOKA separately for SCs with PRI (Preliminary Reverse Impulse) and SCs without PRI . It is found that no PRI appears in SCs larger than 130 nT even in the afternoon side where PRI is more likely to occur. This is interpreted as the strong compression cancel out the magnetic field effect of the PRI current system in large-amplitude SC.

太陽風衝撃波が磁気圏を急圧縮して地磁気急始変化 (SC) が生じる時，圧縮が強ければ，磁気圏界面が静止軌道の内側に入って来る事がある．この時には，磁気圏の昼側サイズが半分位に縮小されることになり，SC も大きくなって，通常の中・小振幅の SC とは異なる性質を示すと思われる．この大振幅 SC を解析すれば，通常の SC からは判らない強い圧縮への磁気圏応答を明らかにできるであろう．この予想の下に，大振幅 SC を調べている．

柿岡観測所は 1924 年からの SC のリストを公開している．それによれば，大半の SC の H 成分振幅は 10-30nT の範囲にあり， 50nT 以上の SC は 5 %弱, 100nT 以上は約 1 % (2021 年 3 月までで 18 個), 200nT 以上は 3 個になる．

ここでは，二つの特性に注目する．

1. 大振幅 SC には，最初に短い大パルスを伴うものがある．1868 年以降，3 番目に大きな 1991.3.24SC では，汎世界的に大きくて短いパルス (柿岡で H 成分振幅：202nT，パルス幅：90 秒) が観測された．最大の 1940.3.24SC(柿岡で 273nT 以上)，2 番目に大きい 1960.11.13SC(220nT）の先端部にも大きなパルスが現れているように見える．

階段状の圧縮波が昼側磁気圏を地球方向に伝搬する時には，磁場増加の波面に沿って西向き電場が作られ，これが極電離層に投影されて，PI(Preliminary Impulse) 電流系が作られる (Tamao,1964)．パルス伝搬の場合には，磁場減少波面沿いに東向き電場が付随するから，投影極電場が西向きから東向きに変わり，逆センスの二つの PI 電流系が続いて現れることになる．この考えが妥当な事は，1991.3.24SC の場合に，モデル計算によって確かめられている (長田，1991)．

2. 上記の 3 大 SC には，PI(Preliminary Impulse) が見られない．柿岡の SC の振幅の日変化を，PI 付きのものと PI 無しのものに分けて調べると，PI が現れやすい午後側でも，130nT 以上の SC には，PI がないことが判る．これは，大振幅 SC では，強い圧縮が PI 電流系の磁場効果をかき消す為と解釈される．

R010-24
C 会場 ：11/5　AM2 （10:45-12:30）
11:30〜11:50

過去１万年間に生じた大規模な太陽高エネルギー粒子イベント

#三宅　芙沙 [1)]
(1 名大 ISEE

Extreme solar energetic particle events occurred in the past 10,000 years

#Fusa Miyake[1)]
(1ISEE, Nagoya Univ.

Cosmogenic nuclides such as 14C, 10Be, and 36Cl are produced by galactic cosmic rays and solar energetic particles (SEPs) in the atmosphere. Extreme SEP events can cause an increase in cosmogenic nuclides-production that greatly exceeds background fluctuations. We have searched for signatures of past extreme SEP events by measuring 14C concentrations in tree rings and 10Be and 36Cl concentrations in ice cores. So far, several candidates of extreme SEP events have been reported.

In this presentation, the latest review of the extreme SEP events discovered using cosmogenic nuclides and a search for extreme SEP events over the past 10,000 years will be reported.

R010-25
C 会場 ：11/5　AM2 （10:45-12:30）
11:50〜12:05

#高橋　直子 [1)], 中溝　葵 [1)], 坂口　歌織 [1)], 塩田　大幸 [1)]
(1 情報通信研究機構

Forecast of Geomagnetic Field Disturbances Using the Empirical Model for Space Weather

#Naoko Takahashi[1)], Aoi Nakamizo[1)], Kaori Sakaguchi[1)], Daikou Shiota[1)]
([1]National Institute of Information and Communications Technology (NICT)

The geomagnetic field disturbance is one of the essential parameters for the space weather forecast in terms of the indicator of disturbances of the Earth's magnetosphere. The magnetospheric condition strongly depends on the solar wind variation associated, for example, coronal mass ejection and/or co-rotating interaction region. Particularly, strong solar wind inputs cause a change of the ring current, resulting a magnetic storm that can be detected as a global change of magnetic field both in space and on the ground.

The disturbance field (Dst) index, which is a parameter that measures the magnitude of the ring current, is referred to understand the magnetospheric condition. Although there are some empirical models to estimate Dst index, they have been proposed to clarify the relationship between solar wind and magnetospheric condition for the past magnetic storm. In this study, we aim to adapt the extended Burton's model (Keika et al., 2015), one of the empirical models, to the forecasting of Dst index. We also attempt to estimate K-index from estimated Dst index that commonly used as the criteria for geomagnetic disturbance alerts in Japan.

We perform a few hours forecast evaluation using the DSCOVR spacecraft data as the inputs. The estimated Dst index shows a good correlation with the observed Dst index for both the main and recovery phases, particularly during strong magnetic storms. However, the abrupt change such as sudden commencement at the beginning of magnetic storm cannot be reproduced well due to the limitation of time resolution. We also estimate K-index using the Dst index and compare with the K-index calculated from the geomagnetic field variation at Kakioka (called as Kakioka K-index). The estimated K-index overestimates comparing with Kakioka K-index because the Dst index is derived from geomagnetic field variation observed at defined four low latitude stations. We also perform a few days forecast evaluation using SUSANOO-CME data as the inputs. The decrease of Dst index estimated from SUSANOO-CME data is reproduced though it is smaller than that of the observed Dst index.

We are planning to adapt the empirical model proposed in O'Brien and McPherron (2000) to estimate the Dst index variation associated with minor-to-moderate magnetic storms. We will discuss the forecast accuracy in this presentation.

R010-26
C 会場 ：11/5　AM2 （10:45-12:30）
12:05〜12:20

#宗像　一起 [1)], 小財　正義 [2)], 加藤　千尋 [1)], 片岡　龍峰 [3)], 門倉　昭 [2,3)]
([1] 信州大・理,[2]PEDSC/ROIS-DS,[3] 極地研

Bidirectional cosmic-ray anisotropy observed with world-wide networks of neutron monitors and muon detectors in November, 2021

#Kazuoki Munakata[1)], Masayoshi Kozai[2)], Chihiro Kato[1)], Ryuho Kataoka[3)], Akira Kadokura[2,3)]
([1]Physics Department, Shinshu Univ.,[2]PEDSC/ROIS-DS,[3]NIPR

We analyze the cosmic-ray variations during a significant Forbush decrease observed with world-wide networks of ground-based neutron monitors and muon detectors during November 3-6, 2021. Utilizing the difference between primary cosmic-ray rigidities monitored by neutron monitors and muon detectors, we deduce the rigidity spectra of the cosmic-ray density (or omnidirectional intensity) and the first- and second-order anisotropies separately, each as a function of time. A clear two-step decreases is seen in the cosmic-ray density with the first 2 % decrease after the interplanetary shock arrival followed by the second another 5 % decrease inside the magnetic flux rope (MFR) at 15 GV. Most strikingly, a large bidirectional streaming along the magnetic field is observed in the MFR with a peak amplitude of 5 % which is comparable to the total density decrease inside the MFR. The peak anisotropy and density depression in the flux rope are both consistent with the rigidity spectrum inversely proportional to the rigidity, which is expected from the betatron deceleration selectively working on non-zero pitch angle particles. The spectra outside the MFR varies dynamically indicating that the temporal variations of density and anisotropy look different in neutron monitor and muon detector data. This is the first attempt to quantitatively deduce the rigidity spectra by analyzing the neutron monitor and muon detector data together.

R010-P01
ポスター 3 ：11/6　AM1/AM2 （9:00-12:30）

コード間結合フレームワークを用いた人工衛星帯電解析の技術基盤開発

#砂田　洋平 [1,2)], 三宅　洋平 [2)], 中澤　和也 [2)], 深沢　圭一郎 [3)], 南里　豪志 [4)], 加藤　雄人 [5)]
([1] 神戸大学システム情報学研究科,[2] 神戸大学,[3] 京大・メディアセンター,[4] 九大・情報基盤セ,[5] 東北大・理・地球物理

Development of Space-Weather-Aware Satellite Charging Analysis Platform based on Code-to-Code Coupling Framework

#Youhei Sunada[1,2)], Yohei Miyake[2)], Kazuya Nakazawa[2)], Keiichiro Fukazawa[3)], Takeshi Nanri[4)], Yuto Katoh[5)]
([1]Kobe University Graduate School of System Informat,[2]Kobe Univ.,[3]ACCMS, Kyoto Univ.,[4]RIIT, Kyushu Univ.,[5]Dept. Geophys., Grad. Sch. Sci., Tohoku Univ.

Space is filled with ionized gas referred to as a plasma originating from the solar wind and ionosphere. The satellite surfaces that are in contact with the plasma collect electric charges of electrons and ions and get charged electrically. Although the satellite equilibrium potential is determined by the current balance onto the satellite among charged particle species, space environmental disturbances such as solar flares and magnetic storms perturb the balance significantly and cause anomalous charging. A number of satellites suffered from such anomalous charging, including the total loss of the U.S. communications satellite Galaxy-15 due to enhanced hot electron inflows associated with a magnetic storm. The precise predictions of satellite have been one of the social significances as one component of space weather forecasting. In this study, we develop a simulation platform that couples the dynamics of the Earth's magnetosphere and satellite charging phenomena based on our in-house code-to-code coupling framework named CoToCoA (Code-To-Code Adapter). In this method, two physical models with different spatial/temporal scales, i.e., a global MHD simulation of the Earth's magnetosphere and a satellite charging analysis based on the OML (Orbital Motion Limited) theory, are coupled with each other by exchanging appropriate physical information. They can be executed as a single MPI parallel program that encompass the above model calculations as its subcomponents. It is expected that the approach enables us to analyze satellite charging phenomena in consideration of magnetospheric environmental changes as well as to achieve efficient use of modern supercomputers.The major research target is to clarify how the satellite potential responses to the changes in plasma environmental and sunlight conditions in a few seconds to a few hours in order to clarify environmental conditions that may cause satellite anomalies. This presentation will focus on our approach and its validity for coupling magnetospheric MHD calculations with satellite charging calculations, which involve totally different time scales.

宇宙空間は太陽風や電離圏を起源とする電離気体・プラズマで満たされており、このプラズマが人工衛星に衝突することで、衛星表面は常に帯電している。衛星帯電値は衛星に流入する荷電粒子フラックスの粒子種間バランスによって決定されるが、太陽フレアや磁気嵐などの宇宙環境じょう乱時には、この粒子フラックスバランスが大きく変動し、異常な衛星帯電が発生することが知られている。近年でも、米国の通信衛星「Galaxy-15」が、磁気嵐時の熱電子流入と帯電により制御不能に陥ったのを初め、帯電が原因とみられる衛星障害は数多く確認されている。衛星帯電を正確に予測し、未然に対策を講じることは、地球電磁気環境の変動を予測する宇宙天気予報における重要な社会的意義の一つである。本研究では我々が独自に共同開発を進めているコード間結合フレームワーク CoToCoA（Code-To-Code Adapter) を用いて、地球磁気圏ダイナミクスと人工衛星帯電現象を連携したシミュレーションプログラムを開発し、連成解析を実施した。本アプローチでは、地球磁気圏グローバル MHD シミュレーションと、軌道運動制限理論に基づく人工衛星帯電解析という、時空間スケールが大きく異なる 2 種類の物理モデルを、適切な物理情報の交換により互いに連結することで、双方の計算をサブコンポーネントとして包含する MPI 並列計算プログラムとして構成する。これにより、スーパーコンピュータの計算能力を有効活用しつつ、磁気圏変動効果を考慮した人工衛星帯電解析が可能になると期待される。数秒から数時間単位で推移する、磁気圏プラズマ環境や日照条件の変動が人工衛星電位に如何なる影響を及ぼしうるかを明らかにすることで、衛星障害が発生しやすい環境条件を導き出すことが本研究の最終的な目的である。本発表では、時間刻み幅が大きく異なる磁気圏 MHD 計算と衛星帯電計算の連携方法に焦点を当て、現在開発中の連成シミュレーションモデルの設計指針とその妥当性を議論する。

R010-P02
ポスター 3 ：11/6　AM1/AM2 （9:00-12:30）

月面利用に向けた超小型・高機能な宇宙放射線環境の計測技術構築の基礎研究

#三好　由純 [1)], 笠原　慧 [2)], 中村　紗都子 [3)], 佐藤　達彦 [4)], 臼井　英之 [5)], 原田　裕己 [6)], 西野　真木 [7)], 菅生　真 [8)], 関　華奈子 [9)]
([1] 名大 ISEE,[2] 東京大学,[3]IAR&ISEE,[4] 原子力機構,[5] 神戸大・システム情報,[6] 京大・理,[7]JAXA,[8] 東大・理・地惑,[9] 東大理・地球惑星科学専攻

High-quality and compact space radiation instruments for the development of lunar surface

#Yoshizumi Miyoshi[1)], Satoshi Kasahara[2)], Satoko Nakamura[3)], Tatsuhiko Sato[4)], Hideyuki Usui[5)], Yuki Harada[6)], Masaki N Nishino[7)], Shin Sugo[8)], Kanako Seki[9)]
([1]ISEE, Nagoya Univ.,[2]The University of Tokyo,[3]IAR&ISEE,[4]JAEA,[5]System informatics, Kobe Univ,[6]Kyoto Univ.,[7]JAXA,[8]Earth and Planetary Science, Univ. Tokyo,[9]Dept. Earth & Planetary Sci., Science, Univ. Tokyo

It is essential for future space development to monitor and forecast space radiation. , because space radiation (solar radiation, galactic cosmic rays, and trapped particle in the radiation belts and plasma sheet) is extremely dangerous for manned activities on the Moon through exposure and charging. Therefore, it is very important to develop a compact and power-saving radiation measurement instruments that can be carried on a Moon rover and carried by astronauts. The research group has started development of a new ultra-compact and high-performance radiation measurement instruments in the framework of JAXA's lunar orbit and lunar mission feasibility study, which focus on measurement and assessment of energetic ions for exposure on the Moon and energetic electrons for charging. PS-TEPC (Position Sensitive Tissue Equivalent Proportional Chamber) and Lunar-RIChes (Ring Image Cherenkov Spectrometer) have been developed for ion radiation measurement, and LEXUS (Lunar Electron eXperiment for hUman activities on the lunar Surface) has been developed for electron radiation measurement. In this presentation, we report the outline of the project and the current progress.

月面での有人活動を行う際に、宇宙放射線（太陽放射線、銀河宇宙線、地球磁気圏荷電粒子）は被ばくや帯電を通してきわめて危険な存在であるため、宇宙放射線の様子を定常的に把握し、さらに予測を行っていくことは、今後の宇宙開発にとって必須である。月面における放射線計測は、有人活動が行われるすべての場所を対象に行うことが必要であるため、ローバーへの搭載や宇宙飛行士による可搬性もふまえて、省電力かつ小型の放射線計測装置を開発する意義はきわめて高い。本研究グループでは、月面での被ばくに対するイオン放射線の計測と評価、および帯電に対する電子放射線の計測と評価の観点から、新たな超小型・高機能な計測装置の開発を、JAXA の月周回・月面ミッションフィジビリティスタディの枠組みで開始した。イオン放射線計測については、PS-TEPC(位置有感生体等価比例係数箱)、Lunar-RIChes(月探査機搭載用チェレンコフ検出器)、また電子放射線計測については LEXUS(電子検出器) の開発を行っている。本講演では、計画の概要と現在の進捗について報告する。

R010-P03
ポスター 3 ：11/6　AM1/AM2 （9:00-12:30）

#小原　隆博 [1)]
[(1] 東北大 惑星プラズマ

Multi-spacecraft observations of widespread solar proton transport in the heliosphere

#Takahiro Obara[1)]
[(1]PPARC, Tohoku University

We present multi-spacecraft observations of widespread solar energetic protons and discuss on the proton acceleration and transport in the wide spread events. Based on the list prepared by Dr. Seiji Yashiro from NASA for the past PSTEP-SEP-CDAW2 workshop in 2019; https://sites.google.com/view/pstep-sep-cdaw2/home, we have investigated wide spread solar proton events and found following signature; i.e. heliographic source of the solar proton distributes in a wide range from -180 degrees to 180 degrees with respect to the central meridian longitude. The bottom figure demonstrates the dependence of the onset time delay of the solar proton after the solar flare upon the heliographic position of source flares. Delay time seems shorter for the western source cases than that for eastern source cases. The shortest delay time was 15 min. and the location of source flare was 100 deg. west in this case. These solar proton events associated CMEs, and the speed of the ejected CMS exceeds 900 km/sec for all cases. By using multi-spacecraft observation data, we have examined the deference of onset times at each spacecraft in detail. In some cases, onset times of the arrived solar protons at each spacecraft were quite similar even though the locations of the spacecraft were quite far. Closer inspection revealed that the solar flare occurred around the sector boundary of the solar magnetic field, where the neutral current sheet structure likely exists. When the energetic solar protons are emitted into the heliospheric neutral sheet structure, these solar protons easily spread widely, resulting in the widespread solar energetic protons as shown in the figure.

Figure caption: The dependence of the time-delay of the solar proton arrival after the solar flare upon the heliographic position of source flares.

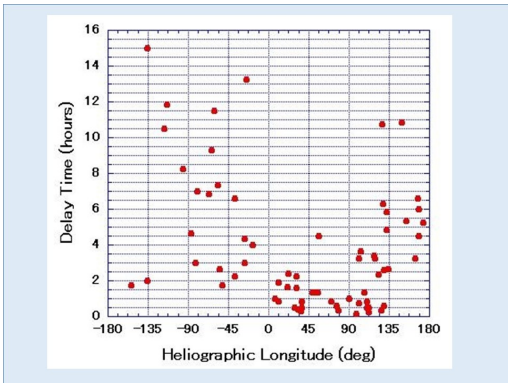

R010-P04
ポスター 3 ：11/6　AM1/AM2 （9:00-12:30）

#中村　雅夫 [1)], 長澤　恒聖 [1)]
([1] 大阪公大・工・航空宇宙

Surface charging plasma environment modeling in the medium earth orbit

#Masao Nakamura[1)], Kosei Nagasawa[1)]
([1]Dept. of Aerospace Eng., Osaka Met. Univ.

The spacecraft surface charging sometimes causes spacecraft anomalies due to electrostatic discharging (ESD). It is important to develop an empirical surface charging plasma environment model in medium earth orbit (MEO). We use electron and proton fluxes from a few eV up to 50 keV measured by the Helium Oxygen Proton Electron (HOPE) and spacecraft potential measured by the Electric Field and Wave instruments (EFW) on the Van Allen Probes from 2012 to 2019. Since the Van Allen Probes are well-designed scientific satellites, their severe charging events are only observed in the eclipse region because of the lack of the photoelectron emission. Therefore we evaluate charging plasma environment features for typical satellites in the daylight and eclipse regions and statistically model their distribution as a function of MLT and L value. The distribution models make it possible to estimate the charging occurrence rate in MEO.

R010-P05
ポスター 3 ：11/6　AM1/AM2 （9:00-12:30）

宇宙天気予報の高度化に向けた最近の国内の動きと NICT の取組

#津川　卓也 [1)]
(1 情報通信研究機構

Recent domestic activities and NICT's efforts for the advancement of space weather forecast

#Takuya Tsugawa[1)]
(1NICT

In recent years, the use of space has been rapidly advancing in the business sector, with the realization of commercial space travel and the advancement of satellite communication plans using commercial small satellite constellations, while solar activity has been gradually increasing in the solar cycle 25. The importance of space weather forecast is increasing in preparation for disasters caused by large-scale space weather phenomena.Under these circumstances, various countries and international organizations, including the United States, the United Kingdom, and South Korea, have been studying the impact of space weather phenomena on social infrastructure and how to respond to them. In Japan, the Ministry of Internal Affairs and Communications held a "Council for the advancement of space weather forecast" from January to June 2022 to discuss the national observation and analysis capabilities and measures for space weather forecast across fields, and published its report on June 21 (https://www. soumu.go.jp/menu_news/s-news/01tsushin05_02000047.html). The report presented the worst-case scenario of an extreme space weather event and made recommendations for crisis management at the national level, including the establishment of alert types and criteria that take into account the magnitude of social impact. In this presentation, I will report on the recent domestic activities for the advancement of space weather forecast and the related efforts of NICT.

第 25 太陽活動周期において、X クラスフレアが複数回観測されるなど徐々に太陽活動が活発化してきている一方、商用宇宙旅行の実現や民間の小型衛星コンステレーションによる衛星通信計画が進むなど、近年ビジネス分野でも急速に宇宙利用が進みつつある。このような状況において、宇宙天気現象の社会インフラへの影響やその対応については、米国、英国、韓国等様々な国や国際機関において検討が進められている。日本においても 2022 年 1 月から 6 月にかけて、総務省「宇宙天気予報の高度化の在り方に関する検討会」が開催され、宇宙天気予報に関して分野横断的に国家としての観測・分析能力や対処の在り方等が検討され、6 月 21 日に報告書が公表された（https://www.soumu.go.jp/menu_news/s-news/01tsushin05_02000047.html）。報告書では、日本では初めてなる極端な宇宙天気現象がもたらす最悪シナリオが示された他、社会的影響の大きさも考慮した新たな警報の種類・閾値の設定など、国家レベルの危機管理に向けた提言がまとめられた。本講演では、このような宇宙天気予報の高度化に向けた最近の国内の動きと、関連する NICT の取組について報告する。

R010-P06
ポスター 3 ：11/6　AM1/AM2 （9:00-12:30）

Van Allen probes 衛星データを用いた電子放射線帯の年変動解析

#中村　紗也 [1)], 大森　和真 [1)], 中村　雅夫 [2)]
([1] 大阪公大,[2] 大阪公大・工・航空宇宙

Study on annual variation of electron radiation belt based on the measurement of the Van Allen probes

#Saya Nakamura[1)], Kazuma Omori[1)], Masao Nakamura[2)]
([1]OMU,[2]Dept. of Aerospace Eng., Osaka Met. Univ.

Understanding the variation of radiation belt electrons is important for spacecraft design and operation of astronaut to evaluate their radiation dose. In this study, we study annual average variations of high energy electron flux observed by the Van Allen probes in 2013-2018. The Relativistic Electron Proton Telescope (REPT) instruments on the Van Allen probes measure electron fluxes in 11 differential channels from 1.5 MeV up to 19 MeV and one higher integral channel. We obtain the following results: (1) the annual average electron flux of the outer radiation belt in the energy range <7.7 MeV was smallest in 2014 during the solar maximum phase: (2) the annual average electron flux of the slot region and nearby outer radiation belt (L <4 Re) in the energy range <7.7 MeV was largest in 2015 when the largest magnetic storm occurred in 2013-2018. We will compare the results with the Akebono satellite data and discuss he long term.

地球近傍の宇宙空間に存在する高エネルギー荷電粒子は宇宙機に作用し，宇宙機の異常動作の原因となることが知られている．放射線帯の高エネルギー電子は人工衛星の内部帯電やトータルドーズ効果による機器劣化や宇宙飛行士の被曝を引き起こす．したがって，電子放射線帯を評価することは今後の宇宙開発において重要な課題である．長年にわたり使用されている電子放射線帯モデルに，NASA で作成された AE-8 があるが，このモデルは近年の観測結果とのずれが指摘されている．また，AE-8 は太陽極大期と太陽極小期の 2 つに分けた経験的な放射線環境を表現する静的モデルであり，太陽活動や地磁気活動による変動に対応していない．これらの変動による影響に対応したモデルを作成するためには，太陽活動と磁気圏・地磁気活動による電子放射線帯の変動を知る必要がある．

本研究では，Van Allen Probes 衛星に搭載されている Relativistic Electron Proton Telescope（REPT）の電子放射線帯の観測データを用いた．REPT は 1.5 MeV から 20 MeV 以上の高エネルギーの電子フラックスを 12 チャンネルのエネルギーに分けて観測した．そのデータを用いて，2013 年から 2018 年の 6 年間について電子放射線帯のエネルギーごとの年平均の変化を調べた．その結果，太陽極大期中の 2014 年は，外帯において 7.7 MeV 以下の電子フラックスが他の年と比較して小さくなっていた．この翌年の 2015 年には，期間中最大の磁気嵐が発生し，放射線帯外帯の 7.7 MeV 以下の電子フラックスが大きくなり，特にスロット領域から L 値が約 4 Re 以下の外帯の内側領域にかけて最大の年となっていた．また，これらの結果を，1989 年から 2015 年に低軌道から放射線帯の観測を行った「あけぼの」衛星の観測データとも比較して長期変動について議論する．

R010-P07
ポスター 3 ：11/6　AM1/AM2 （9:00-12:30）

HF-START プロジェクトにおける HF 帯電波伝搬の際の減衰の評価

#佐藤　駿 [2)], 中田　裕之 [1,2)],Hozumi　Kornyanat[3)], 斎藤　享 [4)], 大矢　浩代 [1,2,5)]
([1] 千葉大・工,[2] 千葉大・工,[3]NICT,[4] 電子航法研,[5] 千葉大・工・電気

Estimation of attenuation of HF radio waves in the simulator for HF-START project

#Shun Sato[2)], Hiroyuki Nakata[1,2)], Kornyanat Hozumi[3)], Susumu Saito[4)], Hiroyo Ohya[1,2,5)]
([1]Chiba University・Engineering,[2]Grad. School of Eng., Chiba Univ.,[3]NICT,[4]ENRI, MPAT,[5]Engineering, Chiba Univ.

HF radio waves propagate through the ionosphere, and are mainly used for long-distance communications, such as aeronautical radio and distant ocean vessel communications. Their propagation path depends on the refractive index in the ionosphere, which is determined by the electron density distribution in the ionosphere. Since the electron density distribution changes from time to time, the distribution of the refractive index also changes with time. HF-START (HF Simulator Targeting for All user's Regional Telecommunications) web service calculates and displays the propagation path of HF radio waves between two arbitrary points using ray tracing. In addition, it provides information such as propagation time and radio waves reflection altitude. The purpose of this study is to add a function to calculate signal intensity of radio waves to HF-START. Currently, we are implementing a function to calculate the attenuation of radio waves necessary to evaluate signal intensity. There are four factors of attenuation to be considered: (1) electron-ion and electron-neutral collisions in the ionosphere, (2) ground reflection, (3) free space path loss, and (4) other factors. The following four factors are considered. Estimation of attenuation (1) uses electron-ion collision frequency, electron-neutral collision frequency, electron temperature, and ion temperature, which are provided by IRI model. The total amount of the attenuation is determined by the integration of the attenuation along the path. The attenuation factors (2), (3), and (4) are estimated by referring to the formulas described in ITU-R P533. The attenuation (2) and (4) are determined to be 2dB per hop and 8.72dB, respectively. In this estimation the attenuation by aurora is not considered because this can be estimated by AE index more correctly as compared to ITU-R P533. We will show the results of the estimation of attenuation in the propagation of the radio waves.

HF 帯電波は電離圏と地上を反射しながら伝搬し、主に国際航空機無線や遠洋船舶通信などの長距離通信に利用されている。その伝搬経路は電離圏における屈折率に依存し、屈折率は電離圏中の電子密度分布によって決定する。電子密度分布は時々刻々と変化するため屈折率も時刻によって変化する。HF-START(HF Simulator Targeting for All user's Regional Telecommunications) の Web サービスは、任意の 2 点間における HF 帯電波の伝搬経路をレイトレーシングにより求めてほとんどリアルタイムで表示し、伝搬時間や電波の反射高度などの情報を提供している。本研究ではユーザーに対して有益な情報として、HF-START に受信強度の計算機能を追加することを目的としている。現在は、受信強度の評価に必要な電波の減衰の計算機能を実装しているところである。考慮する考慮する減衰の要因は以下の４つである。（１）電離層における電子ー イオンと電子ー中性粒子の衝突、（２）地上反射、（３）自由空間経路損失、（４）その他の要因である。減衰 (1) は、電子-イオン衝突周波数、電子-中性粒子衝突周波数、電子温度、イオン温度などを用い、経路に沿った減衰を積分して全体の減衰量を求めている。計算に必要なイオン・電子の密度・温度は IRI モデルにより導出する。(2)、(3)、(4) による減衰は、ITU-R P533 に記載されている計算式を参照して推定する。地上での反射は 1 回あたり 2 dB、その他要因の減衰は 8.72 dB である。オーロラによる減衰は、AE index を用いることで ITU-R P533 による値よりも高精度に求めることが可能になると考えられることから、今回の計算では考慮しないこととする。この計算では 2 点間の伝搬路に沿った減衰のみを考慮し、電離層非一様性による集束/非集束は考慮しないこととする。本発表では、２点間の伝搬における減衰の計算結果を紹介する。

R010-P08
ポスター 3 ：11/6　AM1/AM2 （9:00-12:30）

FMCW イオノグラム画像 E/Es 層エコー検出に関する一般物体検出モデルの高有効性

#廣重　優 [1)], 藤本　晶子 [2)], 阿部　修司 [3)], 池田　昭大 [4)], 吉川　顕正 [5)]
([1] 九工大,[2] 九工大,[3] 九大・i-SPES,[4] 鹿児島高専,[5] 九大/理学研究院

High available of general object detection models for detection of E/Es layer echo on FM-CW Ionograms

#Yu Hiroshige[1)], Akiko Fujimoto[2)], Shuji Abe[3)], Akihiro Ikeda[4)], Akimasa Yoshikawa[5)]
([1]KIT,[2]Kyutech,[3]i-SPES, Kyushu Univ.,[4]KNCT,[5]Kyushu Univ.

Since the sudden changes in the Ionospheric environment can cause some radio disturbance, it is important in space weather forecast to make continual observation of Ionospheric environment in quasi-real time. The purpose of this paper is to propose a highly accurate and robust method for detecting E-layer echoes and sporadic E-layer echoes from Ionogram images. We adopt some existing general object detection methods based on conventional neural network (CNN), and create a deep learning model trained on our own created training data, for our approach to detect E-layer echoes and sporadic E-layer echoes as object instances in an Ionogram image. The main objective of this paper is to reveal the usefulness of the general object detection methods, Faster-RCNN, YOLO and SSD detect E-layer echoes and sporadic E-layer echoes.

In this study, we prepare 1178 Ionogram images (January-December 2019, Sasaguri in Japan, using FMCW Rader) and split them randomly into the training data (942 images) and the validation data (236 images) in the ratio of 8:2 for our experiments. We apply two preprocessing, noise reduction using the bilateral filter which is one of the smoothing filters and smoothing in the horizontal direction, into each Ionogram image. We also perform the annotation process for the training data and give the position information of bounding boxes as the object regions and their class label. Here, the class labels for the E-layers and Es-layers are considered identical.

The results show that the Faster-RCNN and YOLO methods can detect E-layer echoes and sporadic E-layer echoes with high accuracy of 98.96% AP and98.68% AP, respectively, compared to 88.67% AP for SSD (AP is Average Precision: the most commonly used metric is AP for the accuracy of object detection network, derived from precision and recall). The average automatic scaling error of critical frequency foE and foEs was 0.1495, 0.2615, and 0.4373 MHz for Faster-RCNN, YOLO, and SSD, respectively. In addition, using the Faster-RCNN, YOLO and SSD models optimized for E-layer and Es-layer detection from Ionogram images in this study, we confirm that the occurrence distribution of foEs and foEs is consistent with the seasonal and regional occurrence distribution characteristics reported in previous studies.

This study reveals that three general object detection methods used in the experiments are useful for echo region search in Ionogram images. On the other hand, there is still room to reduce the computational complexity of the candidate region search by changing the machine learning network architecture to match the characteristics of each echo, including not only the E-layer echoes but also the normal F-layer echoes or the spread-F echoes during ionospheric disturbances. In the future, we aim to extend the object detection model optimized by Ionogram images as a multi-class classification and regression problem.

R010-P09
ポスター 3 ：11/6　AM1/AM2 （9:00-12:30）

松山　幸生 [1)],#藤本　晶子 [1)]
([1 九州工業大学

Proposal for Magnetic Equatorial Electrojet Pattern Recognition Using String Matching

#Yukio Matsuyama[1)], Akiko Fujimoto[1)]
([1Kyushu Institute of Technology

In recent years, research applying AI and machine learning has increased in the solar-terrestrial science field. This trend suggests that space weather informatics will receive more attention. We investigate the properties of geomagnetic equatorial electrojet (EEJs) in relation to the formation and disappearance of plasma bubbles. We propose a pattern search method that applies string matching as a method to detect cases that match a specific EEJ pattern from a large data archive. In this study, we apply string matching to classify the characteristics of geomagnetic variation, which is numerical data, into an increase and a decrease in the range above and below the quiescent state, and perform feature retrieval using character strings. The Rabin-Karp method is used as the string matching algorithm. The Rabin-Karp method is one of the string matching algorithms based on hash functions, and is used to match multiple character strings with the target string. This method is less computationally expensive and faster to detect than machine learning such as neural networks.

R010-P10
ポスター 3 ：11/6　AM1/AM2 （9:00-12:30）

#池田　昭大 [1)], 魚住　禎司 [2)], 吉川　顕正 [3)], 藤本　晶子 [4)], 阿部　修司 [5)]
([1] 鹿児島高専,([2] 九大・イクセイ,([3] 九大/理学研究院,([4] 九工大,([5] 九大・i-SPES

Schumann resonance parameters at Kuju during intense solar activity

#Akihiro Ikeda[1)], Teiji Uozumi[2)], Akimasa Yoshikawa[3)], Akiko Fujimoto[4)], Shuji Abe[5)]
([1]KNCT,([2]ICSWSE, Kyushu Univ.,([3]Kyushu Univ.,([4]Kyutech,([5]i-SPES, Kyushu Univ.

The Schumann resonance (SR) is the global resonance of electromagnetic waves generated by global lightning activity. SR parameters, which are amplitude and frequency, reflect the properties of both global lightning activity and the state of the Earth-ionosphere cavity. In this study, we investigated relationship between SR parameters and intense solar activities in Oct. and Nov. 2003.

We examined fundamental mode of the SR at Kuju, Japan (KUJ, M.Lat. = 23.4 degree, M. Lon. = 201.0 degree) by comparing solar X-ray, EUV and Proton flux. SR was obtained by an induction magnetometer, which is a part of activities by International Research Center for Space and Planetary Environmental Science, Kyushu University. The data of X-ray and Proton flux were obtained by the GOES series of the satellites on a geostationary orbit. The EUV data were obtained by SEM/SOHO at the Lagrangian point L1.

The long-time enhancement of solar X-ray flux occurred on 18 October, 2003. The enhancement lasted for about 19 days until it recovered to a previous level. SR frequency in H (horizontal northward component) also increased and well followed the X-ray flux. Since X-ray contributes the most to ionization of Earth's ionosphere, we suggested that the increase of SR frequency reflected the density variation of the lower ionosphere. In addition, the effect on SR frequency was not related to the local time at the observatory. The effect on SR seems to be the global character.

We further found that increase of the SR frequency in H often associated with flares. Since X-ray and EUV of flares enhance the ionization of Earth's ionosphere, the variation of the SR frequency seems to reflect the electron density in the ionospheric D-region. We also found that flare-associated variation of SR in H did not depend on local time at the observatory. On the other hand, SR in D (horizontal eastward component) shows local time dependence for flare events.

For SPEs (solar proton events), the variation of the SR frequency in D corresponded with enhancement of the Proton flux (40-80 MeV). It is assumed that the SR frequency in D component relates to the polar ionosphere which is strongly affected by solar proton events. We conclude that SR reflects conditions of the lower ionosphere during the intense solar activity.

R010-P11
ポスター 3 ：11/6　AM1/AM2 （9:00-12:30）

Solar-C (EUVST)/The Solar Spectral Irradiance Monitor (SoSpIM) による宇宙天気研究

#渡邉　恭子 [1)],Harra　Louise[2)],Alberti　Andrea[2)], 今田　晋亮 [3)], 原　弘久 [4)], 清水　敏文 [5)], 川手　朋子 [6)], 三好　由純 [7)], 西谷　望 [7)], 堀　智昭 [7)], 陣　英克 [8)], 垰　千尋 [8)]
([1] 防衛大,([2]PMOD/WRC,([3] 東大,([4] 国立天文台,([5] 宇宙研,([6] 核融合研,([7] 名大 ISEE,([8] 情報通信研究機構

Space weather research with Solar-C (EUVST)/The Solar Spectral Irradiance Monitor (SoSpIM)

#Kyoko Watanabe[1)], Louise Harra[2)], Andrea Alberti[2)], Shinsuke Imada[3)], Hirohisa Hara[4)], Toshifumi Shimizu[5)], Tomoko Kawate[6)], Yoshizumi Miyoshi[7)], Nozomu Nishitani[7)], Tomoaki Hori[7)], Hidekatsu Jin[8)], Chihiro Tao[8)]
([1]NDA,([2]PMOD/WRC,([3]The Univ. of Tokyo,([4]NAOJ,([5]ISAS/JAXA,([6]NIFS,([7]ISEE, Nagoya Univ.,([8]NICT

The Solar Spectral Irradiance Monitor (SoSpIM) has been developed by the Physical Meteorological Observatory in Davos World Radiation Center (PMOD/WRC) in Switzerland to be installed on the Solar-C (EUVST), the next solar observation satellite.

SoSpIM has two observation wavelength bands (170-215A, 1115-1275A) that are also covered by Solar-C(EUVST). By having a redundant system with three independent channels for each wavelength band, the instrument can monitor the degradation and contamination of Solar-C(EUVST). SoSpIM is expected to be used for calibration of the Solar-C(EUVST).

The extreme ultraviolet (EUV) emissions observed by SoSpIM play a main role in controlling the composition of the Earth's upper atmosphere. Both wavelength bands are mainly absorbed in the thermosphere and ionosphere, which are usually formed at altitudes $>$80 km, and are thought to change the composition of the Earth's atmosphere around this altitude. In particular, it is known that sudden fluctuations in EUV emissions due to solar flares greatly change the composition and height profile of the ionosphere, causing space weather phenomena such as communication failures. Therefore, we set up the international SoSpIM science team to study not only solar flare physics, but also discuss what kind of space weather research is feasible using SoSpIM data. In particular, the Japanese members are expected to study the effects of solar emissions on the Earth's ionosphere by comparing the data with observations (e.g. SuperDARN) and model calculations (GAIA) of the Earth's ionosphere.

In this presentation, we will report on the current development status of SoSpIM and the scientific topics considered to be contributed by SoSpIM data.